

IISER PUNE

Effect of intrinsic and extrinsic noise
on a network motif of mutually
inhibiting neurons

Author:

Subhadra Molashe

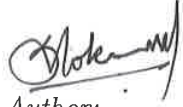
Supervisor:

Dr. Suhita Nadkarni



CERTIFICATE

This is to certify that this dissertation entitled "Effect of intrinsic and extrinsic noise on a network motif of mutually inhibiting neurons" towards the partial fulfilment of the BS-MS dual degree programme at the Indian Institute of Science Education and Research, Pune represents study/work carried out by Subhadra Mokashe at IISER Pune under the supervision of Dr. Suhita Nadkarni, Assistant Professor, Division of Biology, IISER Pune during the academic year 2016-2017.



Author:
Subhadra Mokashe



Supervisor:
Dr. Suhita Nadkarni

डॉ. सुहिता नाडकर्णी / Dr. Suhita Nadkarni
सहायक प्राध्यापक / Assistant Professor
भारतीय विज्ञान शिक्षा एवं अनुसंधान संस्थान
Indian Institute of Science Education & Research
पुणे / Pune - 411 008, India

DECLARATION

I hereby declare that the matter embodied in the report entitled "Effect of intrinsic and extrinsic noise on a network motif of mutually inhibiting neurons" are the results of the work carried out by me at the Division of Biology, Indian Institute of Science Education and Research, Pune, under the supervision of Dr. Suhita Nadkarni and the same has not been submitted elsewhere for any other degree.



Author:
Subhadra Mokashe



Supervisor:
Dr. Suhita Nadkarni

डॉ. सुहिता नाडकर्णी / Dr. Suhita Nadkarni
सहायक प्राध्यापक / Assistant Professor
भारतीय विज्ञान शिक्षा एवं अनुसंधान संस्थान
Indian Institute of Science Education & Research
पुणे / Pune - 411 008, India

ACKNOWLEDGEMENTS

I am deeply grateful to Dr. Suhita Nadkarni for her constant support, inspiration, and insights. She has been extraordinarily supportive and tolerant, and it was possible to finish this dissertation because of her continuous optimism in this work. I would like to thank Dr. Collins Assisi for his invaluable help and feedback. I am thankful to Dr. Chetan Gadgil for his feedback and encouragement. Special thanks to my friends Vidya and Neena for always being there for me. I would like to thank my parents and my brother for having faith in me. I would also like to thank Nadkarni lab and Assisi lab members for being wonderful labmates who have helped, corrected and encouraged me through this journey.

Abstract

Mutually inhibiting neurons is a common motif across many systems like Hippocampus, CPGs(Central Pattern Generators) and Olfaction. Their synaptic interaction ensures that they show alternating activity. The frequency of switching from an active to a quiescent period is a function of the biophysical properties of ion channels present in the neurons, synaptic interaction timescales, network properties, the stimulus and possibly channel fluctuations from a small number of channels. Switching allows neurons to associate with different networks and coordinate patterns of activity that may be relevant for function. The frequency of switching dictates the sequential order of activity of neurons required for locomotion, for example in Lamprey. In this context, reliable switching might be a critical functional requirement. How do networks of mutually inhibiting neurons, a simple most functional module of switching, achieve this reliability despite a noisy framework and environment? We have developed a conductance-based model of two mutually inhibiting neurons wherein inherent switching takes place via a potassium current, sAHP that is triggered by calcium ions. We systematically study the effect of various sources of noise including channel conductance noise, and input noise on switching and robust generation of sequences. Our results show that switching frequency can be tuned with noise amplitude of the extrinsic noise. It has been previously shown that calcium channel fluctuations are the largest contributors of stochasticity at the synapse. As a control simulation experiment, we isolate contributions of calcium channel fluctuations. In this framework, only the calcium dynamics is modeled with a Markovian scheme, and other components are deterministic. Our results suggest that an optimal number of calcium channels help achieve precise switching. This study sheds light on how channel fluctuations affect the network activity and cannot be ignored a priori when slow decay time scales are involved in the neuronal dynamics. Our understanding of the effects of various sources of noise in this illustrative network motif is likely to be applicable to a wide variety of systems.

Contents

1	Introduction	7
2	Methods	9
2.1	Network model	10
2.2	Hodgkin-Huxley Neuron Model	10
2.3	sAHP channels	11
2.4	Synapse	12
2.5	Voltage gated calcium channels	13
2.6	Modelling calcium dynamics	14
2.7	Modelling channel noise	14
2.8	Calcium channel opening failures	18
2.9	insilico	19
2.10	Analysis	21
3	Results	22
3.1	Characterisation of neuronal and network dynamics	22
3.2	Extrinsic modulation	24
3.3	Intrinsic modulation of switching dynamics	28
4	Discussion	36
4.1	Extrinsic modulation of switching dynamics	36
4.2	Effect of intrinsic noise	37
4.3	Tandem Progression Gillespie Algorithm	38
4.4	Future directions	40
5	References	41
6	Appendix	45

List of Figures

1	Ion channels present in the neurons	7
2	Switching mechanism	8
3	Hodgkin Huxley neuron	11
4	sAHP activation	12
5	Synaptic activation	13

6	VGCC activation	14
7	insilico	20
8	Analysis	21
9	Neuron bifurcation	23
10	Network bifurcation	23
11	Switching frequency dependence on r_b	24
12	Frequency modulation by current	25
13	Effect of noise on switching frequency modulation by current	26
14	Frequency modulation by noise	28
15	Dynamics at different numbers of calcium channels	29
16	Effect of calcium failures on switching dynamics	30
17	Effect of increasing current on switching dynamics with different failure rates	32
18	Dynamics at different numbers of calcium channels for a failure rate 0.3 . . .	33
19	Effect of calcium channel failures on switching dynamics	34
20	Dynamics at different numbers of calcium channels for a per channel failure rate 0.3	35
21	Dynamics at different numbers of AHP channels	35
22	Tandem Progression Gillespie Algorithm	39
23	White and Chow Gillespie Algorithm	39
24	Goldwyn and Shea-Brown Gillespie Algorithm	40
25	r_b and noise	45
26	Resting voltage dynamics	45
27	Unconnected neuron stochastic VGCC dynamics	46
28	Connected neuron stochastic VGCC dynamics	46

1 Introduction

Natural systems are inherently noisy. In the case of neuronal networks, the noise arising from various sources could affect the reliability of neural activity. The motivation to undertake this study results from regular and reliable patterns activity seen in neuronal networks in spite of the noisy frameworks the neurons operate in. To study how neuronal networks achieve robustness to noise and maintain regular activity, we look at the simplest network motif which generates regular patterns of activity: a biophysically detailed model of two mutually inhibiting neurons(Fig. 1). Mutually inhibiting neurons is a common motif across many systems like Hippocampus, CPGs(Central Pattern Generators)(Otto Friesen, 1994) and Olfaction (Daun et al., 2009). This network motif is implicated in keeping up regular activity in networks underlying REM sleep cycle (Lu et al., 2006) and working memory (Myre and Woodward, 1993). We are trying to investigate how does a network motif of two mutually inhibiting neurons maintain regular activity in presence noise from different sources? How noise modulates the network activity of the network motif? Do these neurons achieve robust switching via a mechanism akin to coherence resonance?

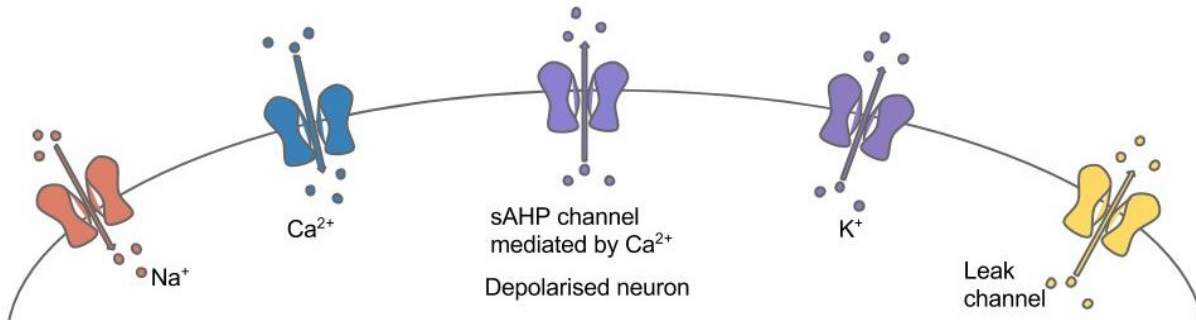


Figure 1: Ion channels present in the neurons.

The synaptic interaction between these two neurons ensures that they show alternating activity. The frequency of switching from an active to a quiescent period is a function of the biophysical properties of ion channels present in the neurons, synaptic interaction timescales, network properties, the stimulus and possibly channel fluctuations from a small number of channels. Switching allows neurons to associate with different networks and coordinate patterns of activity that may be relevant for function. Switching of activity between two neurons dictates the sequential order of activity of neurons required for locomotion, for example in Lamprey (Cangiano and Grillner, 2004) and regularity in switching could be a functional requirement for many systems.

In a network motif of mutually inhibiting neurons, due to the inhibitory coupling, neurons alternate in their activity. The calcium influx from the voltage-gated calcium channels

(VGCC s) mediates the calcium-mediated potassium channels which give rise to a slow after-hyperpolarization (sAHP) current. The slowly deactivating AHP current builds over multiple action potentials and terminates the burst after a characteristic time interval (Manira et al., 2013)(Fig. 2 (a)) which leads to the firing of the other neuron as it is released from inhibition.(Fig. 2 (b)) The slow time-scales of the sAHP current ensure that the switching in the activity takes place after a characteristic time interval (Fig. 2 (a)).

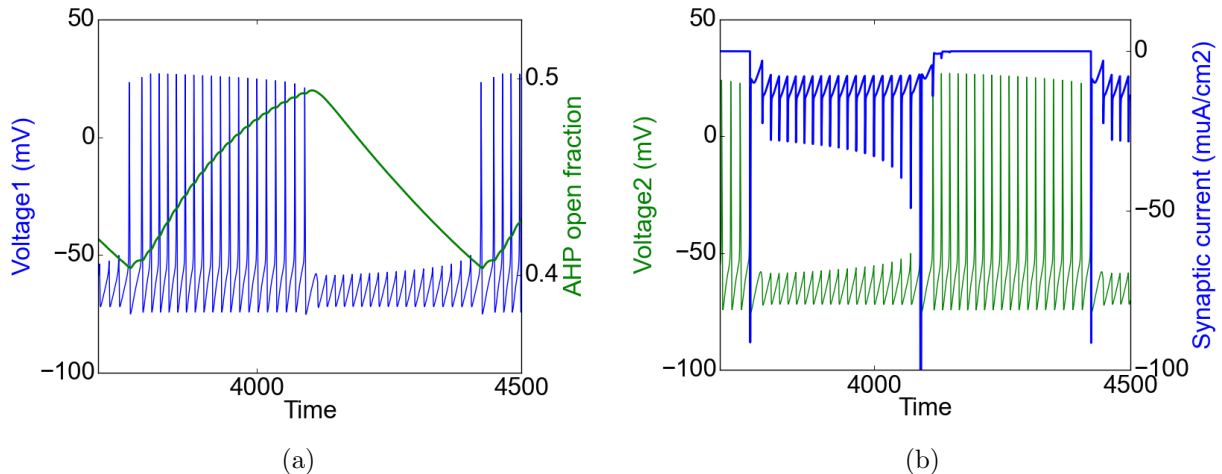


Figure 2: Switching mechanism: (a) Build-up of AHP current over multiple action potentials in neuron 1. (b) Escape from inhibition and burst of the neuron 2.

Noise could disrupt the reliability of neuronal activity, but in many cases, noise can have a co-operative effect on the networks. In neurons, the addition of noise can increase the signal detection and transduction via stochastic resonance (McDonnell and Abbott, 2009; Schmid et al., 2001). Another interesting phenomenon which arises due to the presence of noise and leads to regularity in activity for an optimal level of noise is coherence resonance. Intrinsic channel fluctuations also play an important role in stochastic and coherence resonance and thus cannot be neglected a priori (Schmid et al., 2001). Noise from the voltage-gated channels is crucial to study as it can make subthreshold neuron more excitable and cause suprathreshold activity (White et al., 2000). The low-voltage activated channels which are present in the neurons being studied have been known to have a post-inhibitory rebound effect (Tegnér et al., 1997). Thus it is important to study the effect of noise arising from the stochastic opening of calcium channels on the dynamics of the motif. Due to the slow decay timescales of AHP; each calcium fluctuation is noted and integrated with consecutive calcium fluctuations. This integration property of AHP channels makes the activity of neurons very sensitive to the calcium channel fluctuations.

On the other hand, we investigate how the slow time scales associated with the AHP current can help the network to be robust to the calcium fluctuations and produce regular activity. AHP gating variable due to its slow decay timescales integrates over these fluctuations and generates a less variable AHP current compared to the calcium signal. This integration would help in maintaining regularity in the activity in spite of the noise present. It has been seen that in neurons driven by noisy inputs, multi-scale adaption current can help achieve regularity in oscillations (Nesse et al., 2008b,a). Due to the differences in timescales associated with the calcium and AHP channels, the integration of AHP current over calcium fluctuations would help the neurons achieve regular activity.

We systematically study various sources of noise including channel conductance noise and input noise and its effects on reliability of the network activity. Noise from voltage-gated calcium channels (VGCCs) is one of the largest contributors to the stochasticity at the synapse (Modchang et al., 2010). Our investigations use Markovian framework for simulating channel kinetics dynamics using Gillespie algorithm (Gillespie, 1976) for a realistic description of calcium channel noise. We develop a general framework that includes biophysically detailed, physiological description of channel kinetics to study the effect of noise in transforming activity. Our insight from these studies on various sources of noise in this illustrative network motif is likely to be applicable to a wide variety of systems.

2 Methods

To study the effect of noise on the switching dynamics and how neurons achieve robustness to noise, we have developed a conductance-based model of two mutually inhibiting neurons wherein inherent switching in the activity of neurons takes place via a potassium current, sAHP (slow afterhyperpolarization) current which is mediated by calcium ions. We investigate the role of slow decay time scales associated with the sAHP current in integrating calcium signal generated by the stochastic opening of Voltage-Gated Calcium Channels (VGCCs). Extrinsic noise can be interpreted as the noise arising independently of the state of the neuron, such as background noise. The extrinsic current noise is implemented as an additive term to the differential equation of the voltage. Intrinsic noise can be interpreted as the noise arising from the stochasticity associated with a small number of ion channels and stochastic channel opening. To model realistic intrinsic noise we simulate a Markovian description of the calcium channels using Gillespie algorithm.

2.1 Network model

The neurons have voltage-gated calcium channels and sAHP channels along with voltage-gated sodium and potassium channels and leak current.

$$C \frac{dV_1}{dt} = I_{external} - I_{Na} - I_K - I_{Leak} - I_{synapse} - I_{VGCC} - I_{sAHP}$$

$$C \frac{dV_2}{dt} = I_{external} - I_{Na} - I_K - I_{Leak} - I_{synapse} - I_{VGCC} - I_{sAHP}$$

2.2 Hodgkin-Huxley Neuron Model

The classical Hodgkin-Huxley neuron model describes how action potentials are generated (Hodgkin and Huxley, 1990). It has Na^+ , K^+ and leak channels. The currently accepted model for generation of action potential is given by

$$C \frac{dV}{dt} = -\bar{g}_{Na} m^3 h (V - E_{Na}) I - \bar{g}_K n^4 (V - E_K) - g_L (V - E_L) - I$$

$$\frac{dx}{dt} = \alpha_x (1 - x) - \beta_x x \quad \text{where, } x = n, m, h$$

Where,

V: membrane potential

n,m,h: gating variables which represent the open fraction of channels of sodium(m,h) and potassium(n)

C = 1 $\mu\text{F}/\text{cm}^2$: the capacitance of the cell membrane

$E_{Na} = 50$ mV, $E_K = -77$ mV, and $E_L = -54.4$ mV: reversal potentials of sodium, potassium and leak channels respectively

$\bar{g}_{Na} = 120$ mS/cm^2 and $\bar{g}_K = 36$ mS/cm^2 : maximal conductances of sodium and potassium currents respectively

$g_L = 0.3$ mS/cm^2 : leak conductance

$$\alpha_m = \frac{.1(V + 40)}{1 - \exp(-.1(V + 40))}$$

$$\beta_m = 4.0 \exp(-(V + 65)/18.0)$$

$$\alpha_h = .07 \exp((V + 65)/20.0)$$

$$\beta_h = \frac{1}{1 + \exp((V + 35)/10)}$$

$$\alpha_n = \frac{.01}{1 - \exp(-(V + 55)/10)}$$

$$\beta_n = 0.125 \exp(-(V + 65)/80.0)$$

$$I_{Na} = g_{Na} m^3 h (V - E_{Na})$$

$$I_K = g_K n^4 (V - E_K)$$

$$I_{Leak} = g_{leak} (V - E_{Leak})$$

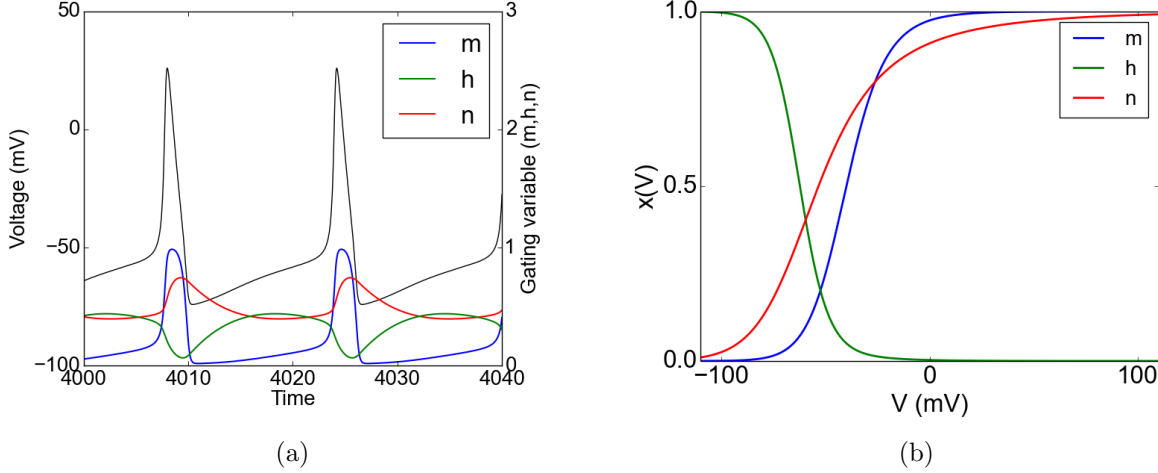
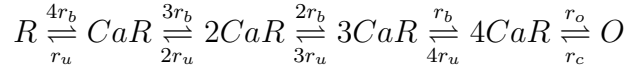


Figure 3: Hodgkin Huxley neuron: (a) The activity of n, m, h gating variables leading to action potentials. (b) Gating variable m,h,n activation as a function of voltage is shown.

2.3 sAHP channels

The sAHP channel model used is a calcium-mediated potassium channel. This model is sAHP channels of CA1 pyramidal neurons (Sah and Clements, 1999) (Stanley et al., 2011).



Where $r_b = 4 \mu\text{M}/\text{sec}$, $r_u = 0.5/\text{sec}$, $r_o = 600/\text{sec}$, and $r_c = 400/\text{sec}$. Here R, CA1R, CA2R, CA3R, CA4R and O are the states of the channel. R is the closed state and O is the open state. The total conductance of the channel is dependent on the fraction of open channels. The rates are calculated with the following assumptions:“

1. The steady-state dose response curve has a steep activation above the resting $[Ca^{2+}]_i$ of 50 nM and has an EC_{50} of 150 nM so that it is efficiently activated by small increases in $[Ca^{2+}]_i$.
2. When $[Ca^{2+}]_i$ falls rapidly, the decay of sAHP is limited by the channel closing and Ca dissociation rates to give a time constant of 1.5 sec, and

3. The peak open probability of the channel is 0.6, and its mean open time is 2.5 msec based on estimates from noise analysis of sI_{AHP} .”

$$I_{sAHP} = g_{sAHP}(V - E_{sAHP})$$

Where $g_{sAHP} = 0.4 \mu\text{S}/\text{cm}^2$ and $E_{sAHP} = E_K = -77 \text{ mV}$

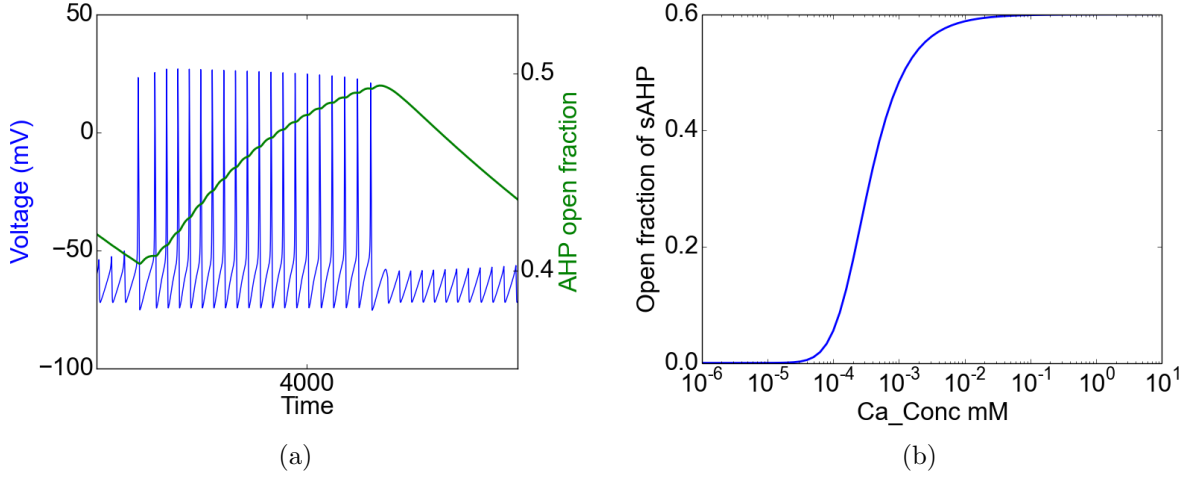


Figure 4: sAHP activation: (a) Slow build-up of AHP open fraction over multiple action potential. (b) Gating variable of the AHP activation as a function of intracellular calcium concentration.

2.4 Synapse

Inhibitory synapses are modelled using a tan hyperbolic function.

$$\rho = \frac{\tanh(\frac{V}{4})}{2}$$

$$\frac{ds}{dt} = \frac{\rho}{\tau_r}(1 - s) - \frac{1}{\tau_d}s$$

$$I_{syn} = \bar{g}_{syn}(V - E_{syn})$$

Where $\bar{g}_{syn} = 2.2 \text{ mS}/\text{cm}^2$ and $E_{syn} = -80 \text{ mV}$.

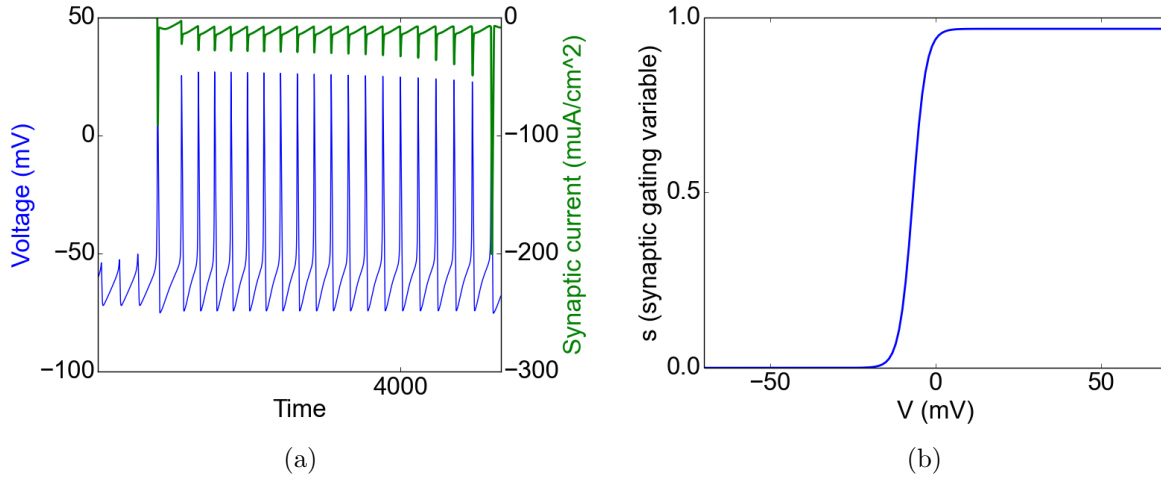


Figure 5: Synaptic activation: (a) The synapse is activated at suprathreshold voltages and follows the voltage trajectory. (b) Gating variable of the synapse activation curve.

2.5 Voltage gated calcium channels

The model used is of L-type $Cav_{1.3}$ calcium channels which open at low voltages (Stanley et al., 2011).

$$\begin{aligned}
 S_0 &\xrightleftharpoons[\beta(V)]{2\alpha(V)} S_1 \xrightleftharpoons[2\beta(V)]{\alpha(V)} S_2 \\
 \alpha(V) &= \frac{\sqrt{x_\infty}}{\tau} \\
 \beta(V) &= \frac{1 - \sqrt{x_\infty}}{\tau} \\
 x_\infty(V[mV]) &= \frac{1}{1 + e^{-\frac{(V+30)}{6}}}
 \end{aligned}$$

Here α, β are voltage dependent probabilities of transitions of states S_i . The conductance is dependent on the fraction of open state.

$$I_{Cav} = g_{Cav}(V - E_{Cav})$$

Where $g_{cav} = 0.15 \text{ mS/cm}^2$ and $E_{cav} = E_{Ca} = 25 \text{ mV}$

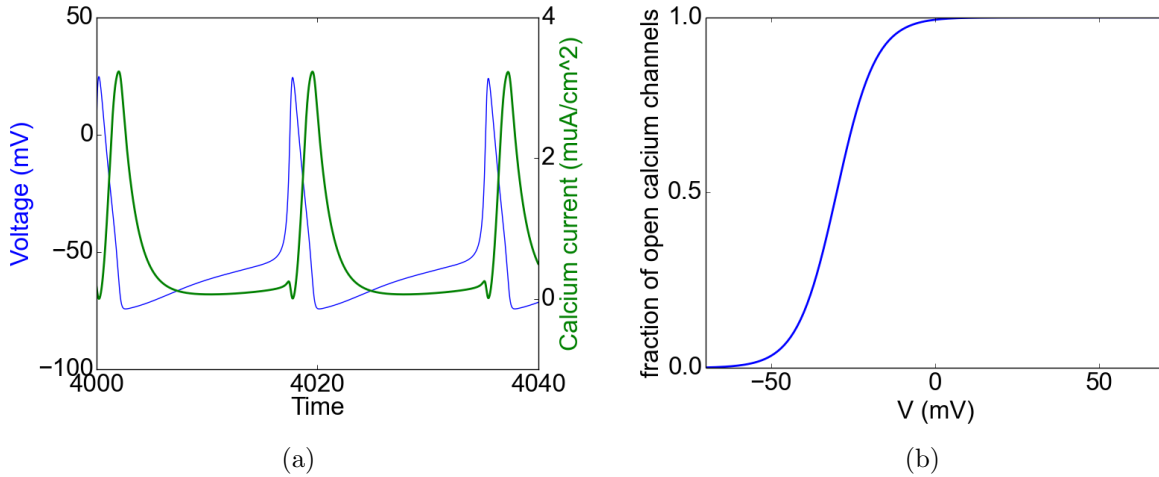


Figure 6: VGCC activation: (a) The opening of VGCCs due to action potentials (b) Gating variable of VGCC activation as a function of voltage.

2.6 Modelling calcium dynamics

The intracellular calcium concentration dynamics is modeled as a leaky integrator (Stanley et al., 2011) (Wang, 1998).

$$\frac{d[Ca^{2+}]}{dt} = (-\alpha I_{Cav}) - \frac{([Ca^{2+}])}{\tau_{Ca}}$$

Where $\alpha = 2.10^{-4}[mM(ms\mu A)^{-1}cm^2]$ and $\tau_{Ca} = 14$ ms. α depends on area to volume ratio of the neuron, intracellular buffering of calcium, and stochasticity factor, and converts calcium current into units of calcium concentration per unit time. The resting calcium concentration is 100 nM and goes upto $2.5 \mu M$ per spike.

2.7 Modelling channel noise

When the number of ion channels from which the neuron reads the ionic currents increases, the fluctuations in the current becomes smaller, and at a very large number of ion channels the ionic currents can be modeled deterministically. In neurons, a small number of ion channels dictate the neuronal dynamics, making it imperative to study how the stochastic ion currents coming in from a small number of ion channels affects the neuronal and network activity. Channel noise has been extensively studied, and various methods to model channel noise have been explored (reviewed in (Goldwyn and Shea-Brown, 2011)), the stochastic dynamics simulated using Gillespie algorithm is considered to be the closest to the real fluctuations observed in neuronal recordings. As a control experiment to study the effect

of noise arising from ion channel fluctuations we implement Markovian description only for calcium or AHP channels using Gillespie algorithm (Gillespie, 1976) whereas the other components of the model are modeled deterministically. We developed a Gillespie-Euler Hybrid Algorithm: Tandem Progression Gillespie (TPG) to simulate realistic time scales and amplitudes of channel noise. Previous algorithms such as the algorithm suggested in the model code from (Goldwyn and Shea-Brown, 2011) updates the voltages when time is an integral multiple of the step size. This algorithm is correct under the assumption that the rates for transitions do not change between two time-steps and there are no slow time-scales involved which could keep track of all the fluctuations, as the fluctuations between the fixed time steps are not seen by the voltage and other currents in the neuron.

Algorithm 1 Goldwyn and Shea-Brown Gillespie Modification

```

1:  $t_s \leftarrow$  time of the next transition
2:  $t_w \leftarrow$  time to the next transition
3:  $t \leftarrow$  current time
4:  $dt \leftarrow$  fixed time step
5: Initialize the state vector for ion channels
6: While ( $t_s < t + dt$ ):
7:   procedure GILLESPIE UPDATE
8:     Calculate rates and total rate for the transtions
9:     Calculate  $t_w$ 
10:     $t_s \leftarrow t_s + t_w$ 
11:   If ( $t_s < t + dt$ ):
12:     update the states return open fraction of channels
13: current = g(Gillespie Update)(V-E)
14: Integrate at  $t = [0, t_{total}, dt]$ 

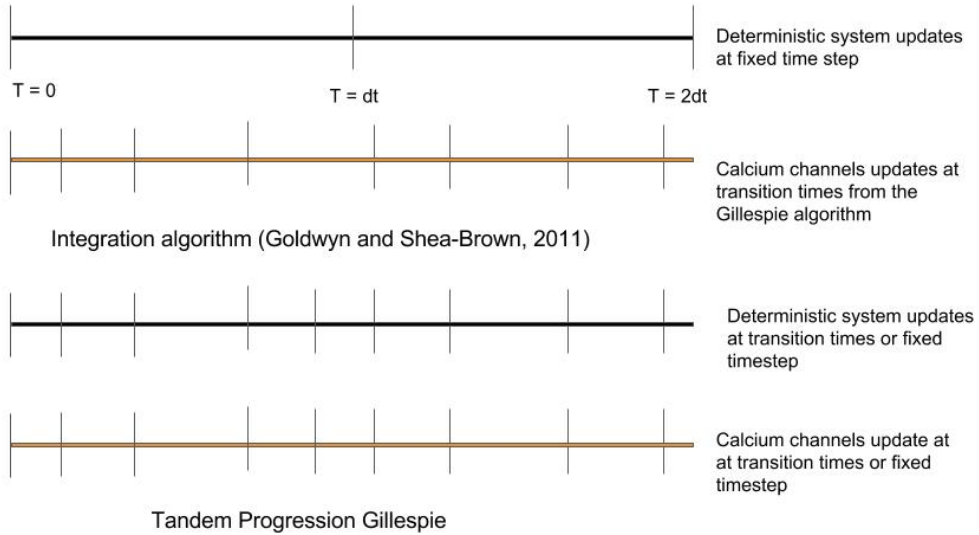
```

Another hybrid algorithm suggested by (Chow and White, 1996) integrates the deterministic system till the waiting time given by Gillespie algorithm and updates the stochastic system only after Gillespie waiting times. When the Gillespie waiting times are smaller than the deterministic time step, the system is integrated at the waiting times. This algorithm assumes that the rate constants do not change during the time step and the rate and waiting time calculations take into account the dynamics and time-scales from all the ion channels present in the neuron.

Algorithm 2 Chow and White Gillespie Modification

```
1:  $t_s \leftarrow$  time of the next transition
2:  $t_w \leftarrow$  time to the next transition
3:  $t \leftarrow$  current time
4:  $dt \leftarrow$  fixed time step
5: Initialize the state vector for ion channels
6: procedure GILLESPIE UPDATE
7: if ( $t == t_s$ ):
8:   Calculate rates and total rate for the transtions
9:   Update the states return open fraction of channels
10:  Recalculate the rates
11:  Calculate  $t_w$ 
12:    $t_s \leftarrow t_s + t_w$ 
13: current = g(Gillespie Update)(V-E)
14:  $dett = \min(t + dt, t_s) - t$ 
15: Integrate  $\frac{dX}{dt} * dett$ 
16:  $t \leftarrow t + dett$ 
```

In our case where we wanted to study the effect of the channel noise arising from one type of ion channels, we could not use any of the previous hybrid algorithms as integrating at fixed time steps will lead to missing channel fluctuations that take place between two time-steps. From our simulations where we had added white noise to the current, it was seen that calcium fluctuations caused by voltage fluctuations are noted by the AHP current and change the switching dynamics significantly. The fast activation and slow decay timescales associated with the AHP current will cause these fluctuations to add up in the AHP current and lead to faster build-up up to the threshold AHP current. Thus it is important not to miss these fluctuations and to achieve this; we update the whole system deterministic as well as the stochastic system at the Gillespie time-steps.



While integrating at these waiting times, which could be very long for small channel numbers, the dynamics of the other components of the model neuron may not be captured correctly and could lead to errors when the waiting times are very long. To model the neuronal dynamics correctly, when the waiting times are larger than a fixed time step (0.01 msec used in simulations) we integrate the system at the fixed time step and also update the stochastic channel states at every integration step to take into account the changed voltage and current values. Thus by updating the whole system together, we believe that we are modeling the stochastic channel dynamics as well as the neuronal and network dynamics accurately.

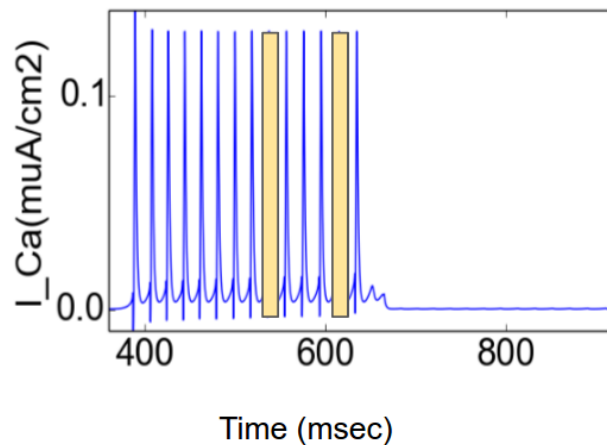
Another approach taken to model channel fluctuations is the system size expansion approach used by (Fox and Lu, 1994) which involves solving the drift-diffusion equation to accurately model the stochastic dynamics simulated using the Gillespie algorithm as the Gillespie algorithm is computationally expensive. Using this approach was not necessary as the system is not large and also would have lead to missing out on accurate time scales of noise. The method we developed is called as Tandem Progression Gillespie as every component of the model is updated at the same time and is described below:

Algorithm 3 Tandem Progression Gillespie

```
1:  $t_s \leftarrow$  time of the next transition
2:  $t_w \leftarrow$  time to the next transition
3:  $t \leftarrow$  current time
4:  $dt \leftarrow$  fixed time step
5: Initialize the state vector for ion channels
6: procedure GILLESPIE UPDATE
7: Calculate rates and total rate for the transtions
8: Update the states return open fraction of channels
9: if ( $t == t_s$ ):
10:   Recalculate the rates
11:   Calculate  $t_w$ 
12:    $t_s \leftarrow t_s + t_w$ 
13: current = g(Gillespie Update)(V-E)
14:  $dett = \min(t + dt, t_s) - t$ 
15: Integrate  $\frac{dX}{dt} * dett$ 
16:  $t \leftarrow t + dett$ 
```

2.8 Calcium channel opening failures

To test how AHP integrates over irregular and unreliable calcium signal we induce calcium channel opening failures with a given probability. Calcium failures are modeled as individual channel failures and as ensemble level or pulse failures.



Modelling calcium pulse failures

Ensemble level failures are calcium pulse failure. Each calcium pulse can be invisible to the neuron and thus AHP current with a certain probability (failure rate). The calcium current comes up again after the failed calcium pulse, and the failure is limited to the duration of calcium pulse and is carried out by multiplying a voltage-dependent block on the calcium current. In this case, all channels fail to open during the block. In the case of an individual channel failure, each channel opening transitions fail with a certain failure probability (failure rate), and thus only one channel fails to open.

2.9 insilico

insilico is a C++ based computational tool specifically designed developed to simulate neurons. The deterministic model is implemented using insilico-0.25. Following is the illustration of the structure and flow of simulations in insilico.

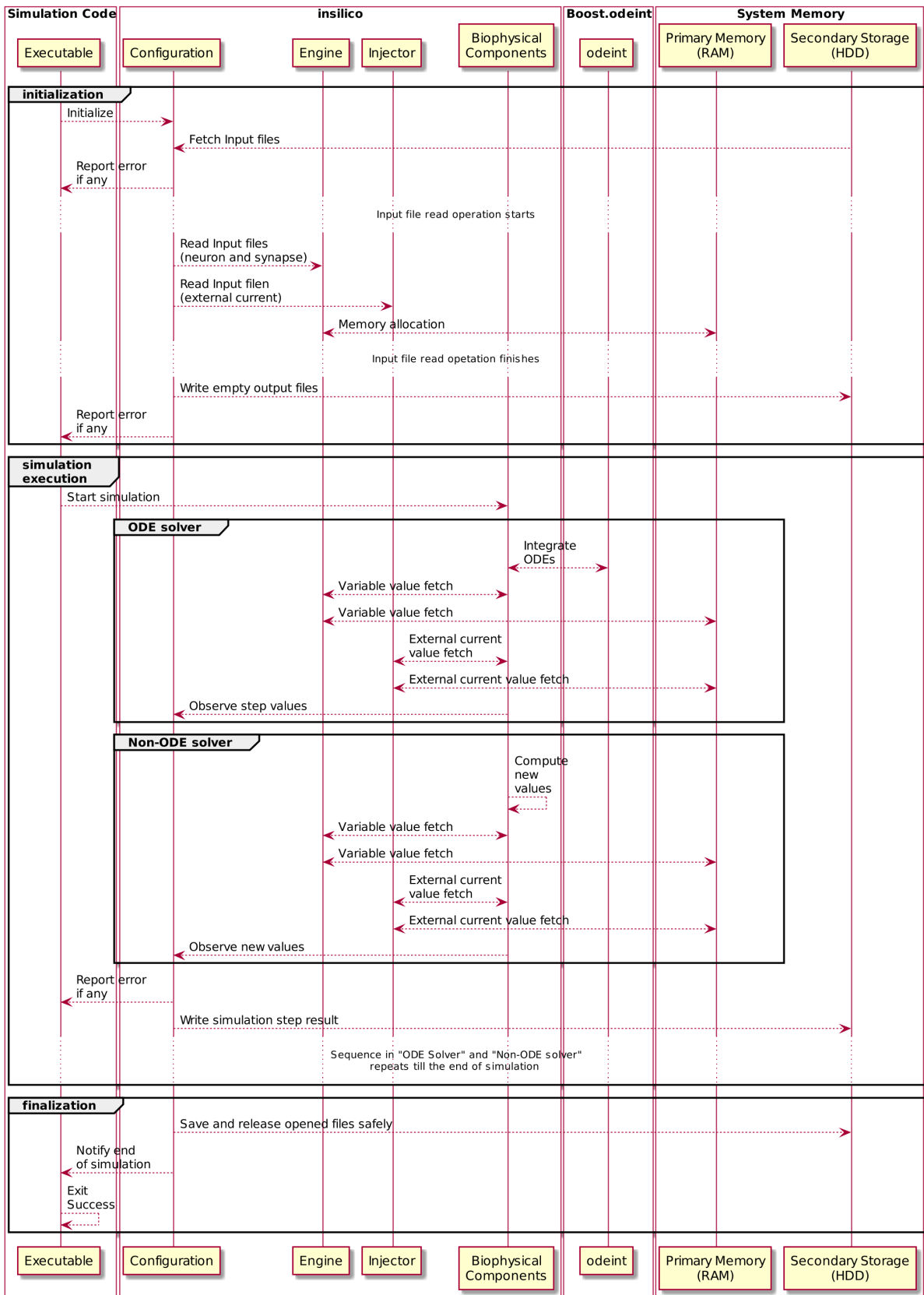


Figure 7: insilico execution and flow. Adapted from <http://www.iiserpune.ac.in/~collins/insilico/>.

2.10 Analysis

To study the effect of various parameter on the switching dynamics, we look at the burst length and the switching frequency of the neurons which is the primary functional read-out of the motif.

Inter-spike interval and Firing frequency: The time difference between peaks of two consecutive action potentials is the inter-spike interval, and multiplicative inverse of the inter-spike gives us the firing frequency of the neuron.

Inter-burst interval and switching frequency: When the burst terminates because of AHP current, and other neuron takes over and inhibits the first neuron, the interval between the last action potential from the last burst to the first action potential of the next burst of the neuron is called interburst interval(IBM). The inverse of IBM is called switching frequency or burst frequency. The action potential is detected if the voltage goes higher than 15 mV and if such a detection happens after minimum of time difference of 15 msec after the last detection. A burst is detected when interspike intervals greater than twice of the last inter-burst interval. To calculate the switching frequency, mean of a fixed number of burst lengths are calculated.

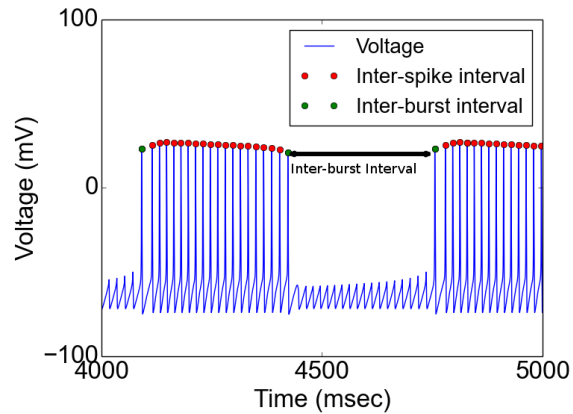


Figure 8: Analysis: Peak detection and burst detection.

As a measure of regularity of bursts coefficient of variation is calculated where T is the interburst interval, is given by

$$CV = \frac{\sqrt{\langle T^2 \rangle - \langle T \rangle^2}}{\langle T \rangle}$$

3 Results

The intrinsic timescales of the ion channels and synaptic connections interact to produce regular network activity. In our context, the slow build of AHP current over multiple action potentials when the network module is driven by external current along with synaptic interaction between two neurons leads to alternation in activity between two neurons (Fig. 2). The characteristic length of the burst is determined by various neuronal and network parameters such as the external current, AHP-calcium binding and unbinding rates, noise levels and synaptic coupling between the neurons. Noise arising from different sources can affect the network dynamics distinctly, and thus effect of each noise source needs to be investigated separately. We investigate the effect of current noise and channel noise on the switching dynamics. It has been shown that the main source of stochasticity at the synapse is calcium channel noise (Modchang et al., 2010). sAHP current which is calcium-mediated potassium current determines the termination of the burst, making it crucial to study calcium channel noise and how AHP current integrates over these stochastic calcium pulses to achieve regular switching. Study of intrinsic noise arising from calcium channel fluctuations involves how changing the level of stochasticity changes the network dynamics, the regularity of switchings and the excitability of the neuron. We study the integrative properties of the AHP by varying the number of calcium pulses the current integrates over by inducing calcium pulse failures. The following sections describe the investigations about extrinsic and intrinsic modulation of the switching dynamics in detail.

3.1 Characterisation of neuronal and network dynamics

Unconnected neuron fires over a large range of values of external current. We look at the bifurcation properties of a biophysically detailed unconnected neuron where the external current is the bifurcation parameter. The neuron undergoes subcritical and supercritical Hopf bifurcation at current $\sim 10 \mu A/cm^2$ and current $\sim 150 \mu A/cm^2$ respectively. The amplitude of oscillations decrease on increasing the current, and the firing frequency increases on increasing the current.

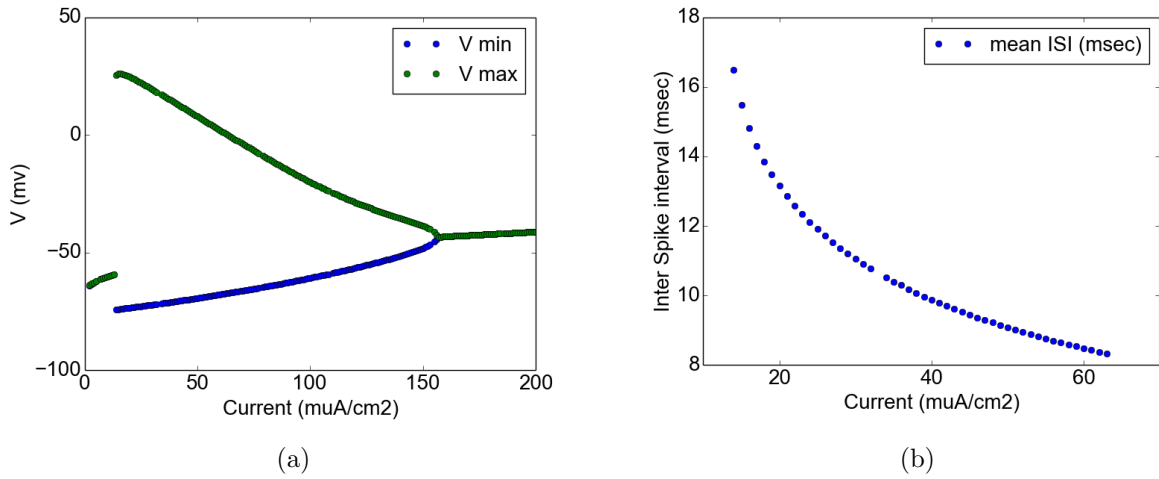


Figure 9: Neuron bifurcation (a) The minima and maxima of voltage observed for varying external current (b) The range of inter-spike interval for the corresponding neuron in (a).

Neurons which are part of the motif of two mutually inhibiting neurons due to the synaptic coupling and characteristic properties of the ion channels present in the neurons show alternating bursting activity for a given range of external current (13 muA/cm^2 to 18.4 muA/cm^2).

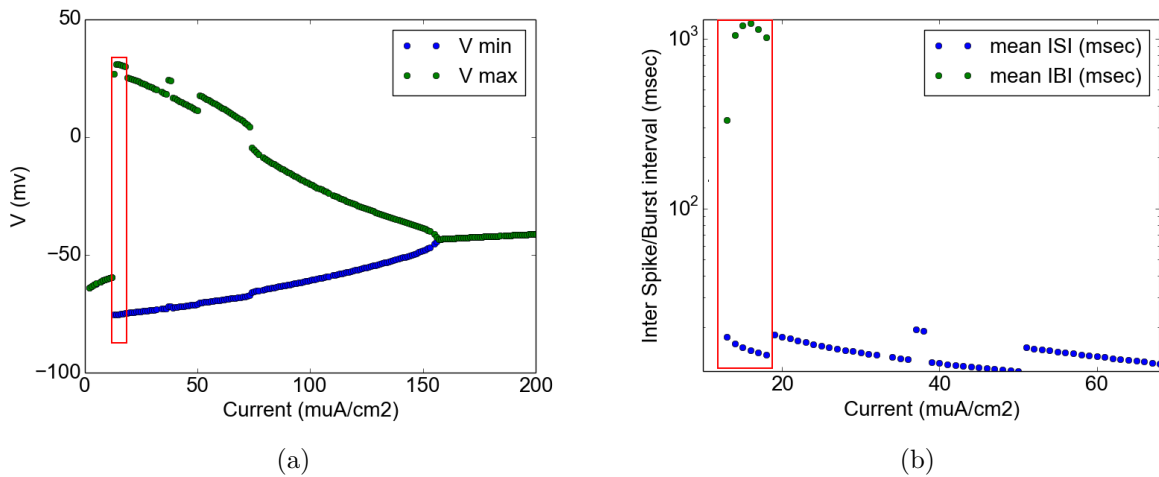


Figure 10: : Network bifurcation (a) The voltage range for varying external current (b) The range of inter-spike and inter-burst interval for varying external current for a neuron from the motif of mutually inhibiting neurons. Range of activity of our interest is enclosed in red boundaries

Dependence of switching frequencies on the AHP-calcium binding rate r_b

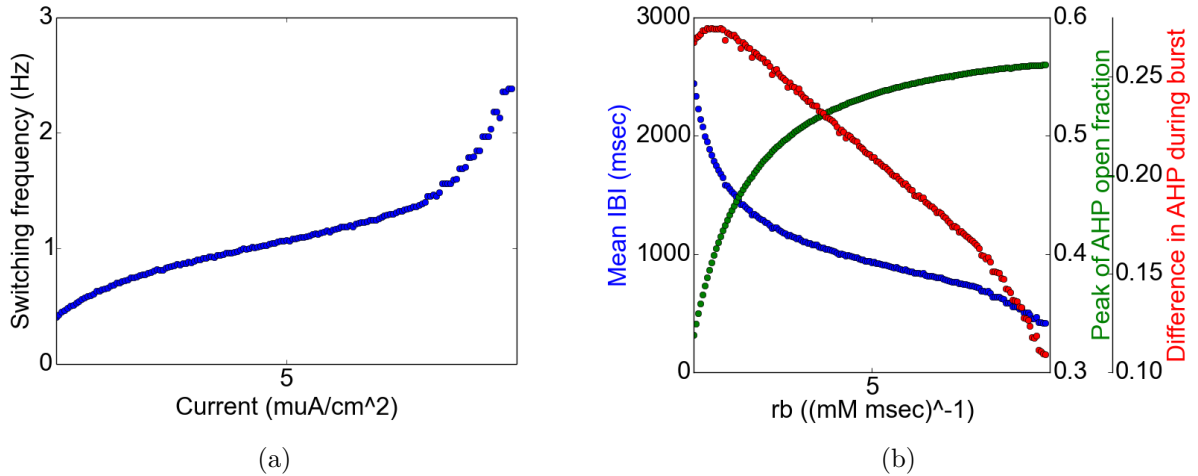


Figure 11: Switching frequency dependence on r_b : (a) The switching frequency increases on increasing r_b (b) The AHP current builds up faster as r_b is increased.

The switching frequency increases on increasing r_b as the AHP is more sensitive to the calcium pulses, which leads to faster build-up for the same level of calcium concentration. The faster build-up of AHP causes the burst to terminate sooner, increasing the switching frequency. For current value of $14 \mu A/cm^2$ the r_b value for which switching is seen is $\sim 1(mM \text{ msec})^{-1}$ to $\sim 9(mM \text{ msec})^{-1}$

3.2 Extrinsic modulation

Modulation of switching frequency by driving current

The neurons we model are not inherent firing neurons and need to be driven by an excitatory input to fire action potentials. For the given set of parameters described in the methods, on increasing the external current, the firing frequency increases (Fig. 12 (b)). The switching frequency shows a non-monotonic trend with increasing current (Fig. 12 (a)) due to two opposite effects increasing current has on the neuronal dynamics. Increasing firing frequency increases the calcium spike frequency (Fig. 12 (c)) which leads to a faster build-up of AHP current. The AHP current has to achieve a higher threshold current to terminate the burst due to increased external current and decreases the switching frequency (Fig. 12 (a)) as it takes longer to reach a higher threshold current (Fig. 12 (a)). When the current is further increased, the increased calcium spike frequency causing a faster build-up of AHP, even though AHP current has to reach a higher threshold value and causes the switching frequency to further increase by increasing the driving current (Fig. 12 (a)).

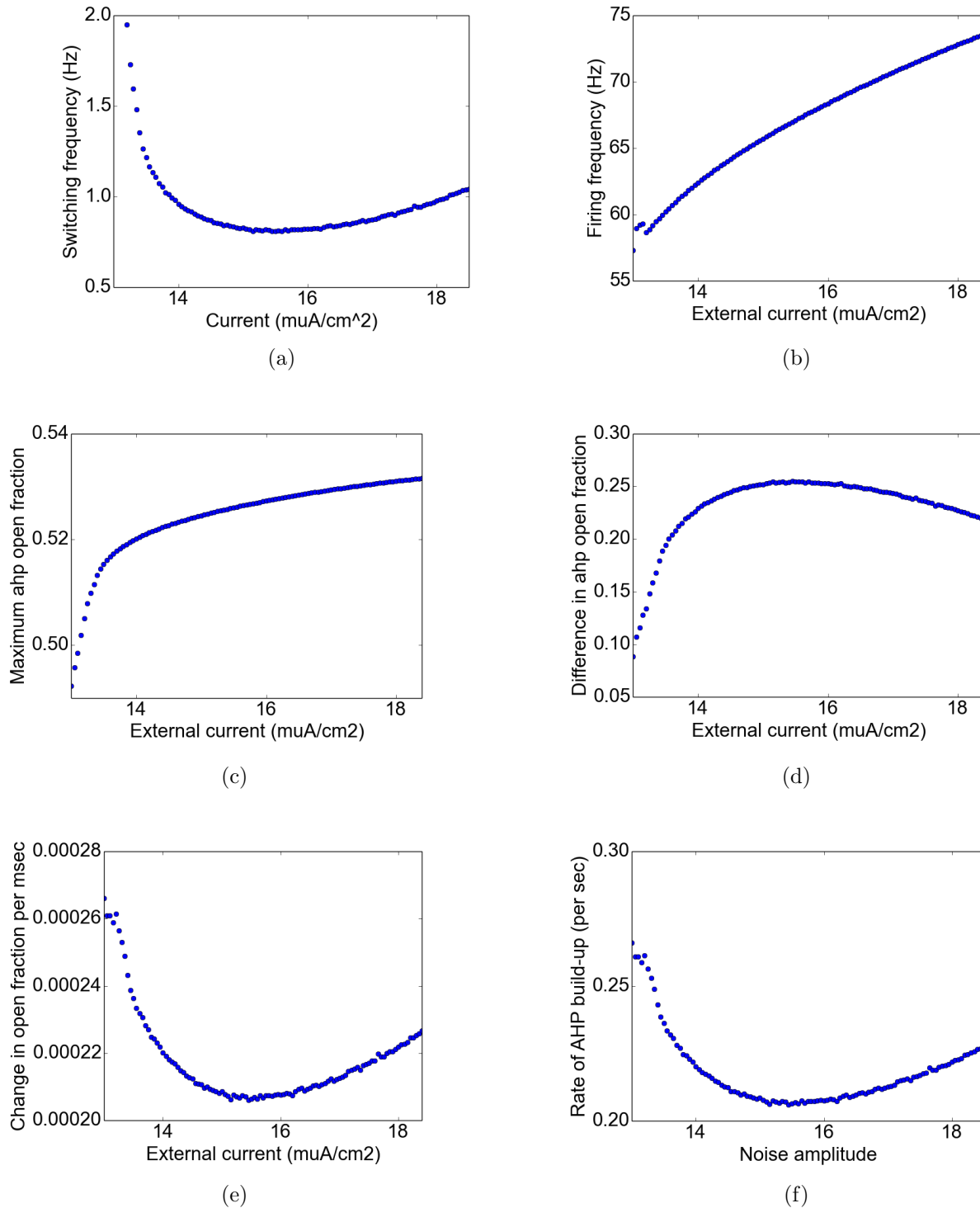


Figure 12: Frequency modulation by current: (a) The switching frequency shows a non-monotonic dependence on the external current (b) The firing frequency increases on increasing the current. (c) The peak AHP open fraction reached increases monotonically on increasing the current. (d) The difference in AHP open fraction during the burst is a read-out of the inter-burst interval of the neuron. (e) The change in the open fraction of sAHP current shows a minimum at an intermediate current value which indicates after which increasing current would increase the switching frequency. (f) The change in AHP open fraction fraction per msec shows a minimum at an intermediate calcium spike frequency.

Intermediate current values show the least change in open fraction per msec or rate of AHP build-up(Fig 12 (e)). For an optimal range of calcium pulse frequency, the change in open fraction per msec or rate of AHP build-up is minimum, suggesting that for a range of optimal frequencies of calcium pulses over which AHP integration could be less to sensitive to fluctuations (Fig 12 (f)). This minimum in AHP build-up rate also suggests that AHP current could also be less sensitive to fluctuations at intermediate current values. To test this, we add a zero mean white noise to the current. A minimum in CV is seen for intermediate currents indicating a range of calcium spike frequencies for which the switchings are robust to noise (Fig 13 (b)). Also for a higher noise amplitude, the switching frequency is higher (Fig 13 (a)).

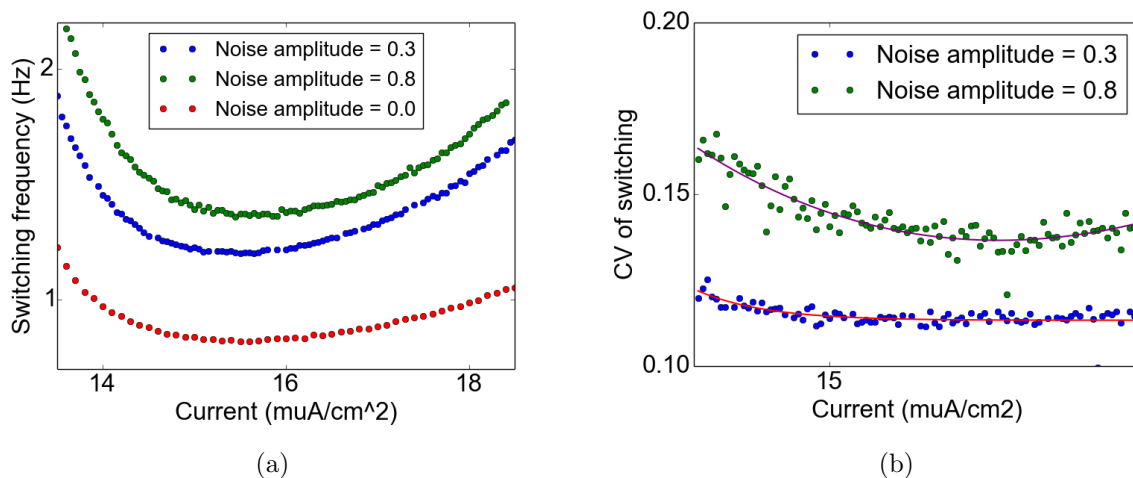
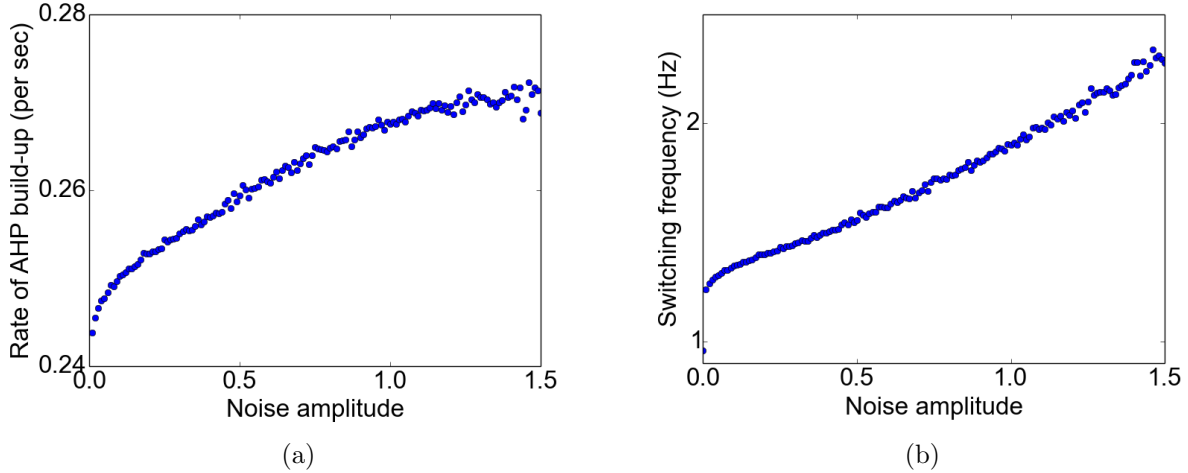


Figure 13: Effect of noise on switching frequency modulation by current: (a) The switching frequency is higher for higher noise levels and even in the presence of different noise levels a non-monotonic dependence on current is seen. (b) The CV shows a minimum at intermediate current values.

Frequency modulation by external noise



Frequency modulation by noise (a) The AHP build-up rate increases on increasing the noise amplitude (b) The switching frequency increases with increase in noise amplitude.

On increasing the noise amplitude, there are larger voltage fluctuations leading to larger fluctuations in the calcium concentration. These larger fluctuations in calcium concentration are noted by the sAHP current due to its fast rise timescale. But as the decay time scales of the AHP current are long (Fig. 4 (a)), the rise in AHP due to calcium fluctuations accumulates over time and leads to a faster build-up of AHP current terminating the burst earlier (Fig. 14 (a)). The CV monotonically increases as the noise amplitude is increased without showing any stochastic resonance-like phenomenon (Fig. 14 (b)) and is not equal to zero at zero noise because of the sampling error.

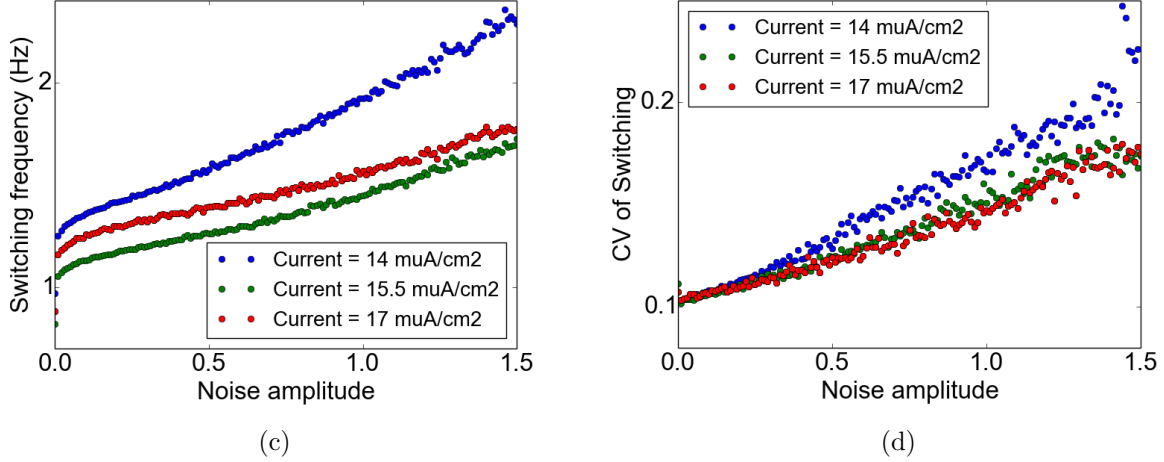


Figure 14: Frequency modulation by noise (a) The switching frequency increases as noise amplitude is increased. (b) The coefficient of variation increases with increase in noise amplitude.

With a small loss of regularity, the addition of noise increases the range of switching frequencies which the network motif can achieve by $\sim 400\%$ (Fig. 14 (a)). In this case, noise is serving as a feature rather than the bug by helping the neurons to achieve switching frequencies which were not possible with only changing the current.

3.3 Intrinsic modulation of switching dynamics

Studies have shown the stochasticity arising from channel fluctuations can change the neuronal excitability, firing thresholds and reliability of neuronal activity (White et al., 2000). It is known that when the number of channels the current is recorded from is increased, the fluctuations in the current from the ion channels become smaller and for very large channel numbers the current can be modeled deterministically (Fig (25)). In neurons, a small number of ion channels dictate the neuronal dynamics, and it is essential to study how the stochastic current from these small number of ion channels determine the switching dynamics. We study the effect of channel noise by systematically varying the number of ion channels present in the neuron by keeping the total flux through all the ion channels constant. Due to the slow time scales associated with the AHP current which is a calcium-mediated potassium current, it is sensitive to the calcium fluctuations which arise due to VGCCs channel fluctuations and has a long memory of these fluctuations. We study the effect of calcium channel noise and AHP channel noise separately. To study the effect of the stochastic opening of calcium channels which known to be the biggest contributor to the stochasticity in neurons, we first implement VGCC's Markovian description using Tandem

Progression Gillespie algorithm as described in methods.

Effect of calcium channel noise on the switching dynamics

For an unconnected neuron at a current constant of $14 \mu A/cm^2$ and constant calcium channel conductance of $0.15 mS/cm^2$ increasing the number of calcium channels decreases the stochasticity in calcium channel opening (Fig. 26). With TGP we see that the open fraction reaches higher open fraction than the deterministic case for a small number of channels (Fig. 28).

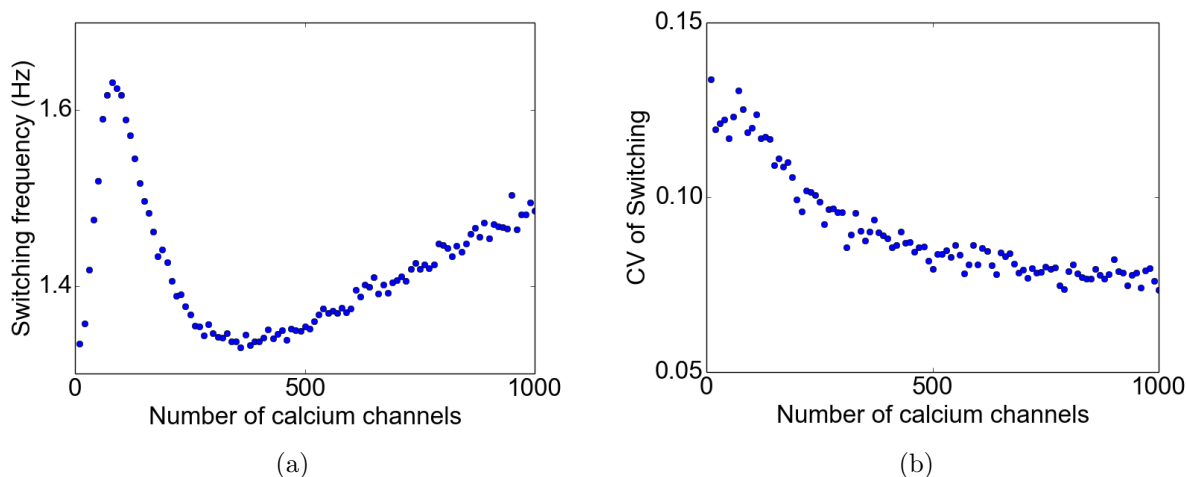


Figure 15: Dynamics at different numbers of calcium channels. (a) Variation in switching frequency due to changing the number of calcium channels (b) CV of inter-burst intervals for varying the number of calcium channels.

For a connected neuron, we see that the switching frequency follows a non-monotonic trend with increasing VGCCs (Fig. 15 (a)). The CV of switching decreases with increasing channel numbers (Fig 15 (b)). The switching frequencies are proportional to the peak open fraction achieved during calcium pulse (Fig. 15 (a)) and (Fig. 28 (a)). The fluctuations become smaller, and the switching frequency decreases as the number of VGCCs is increased (after 100 channels). The waiting times from the Gillespie algorithm become shorter as the number of VGCCs are increased. When the number of VGCCs is further increased the fluctuations become smaller but happen more often. Due to the slow time-scales of the AHP current, these closely spaced fluctuations add up in AHP current leading to a faster build-up of AHP current. Due to increasing frequency and decreasing amplitude of fluctuations with increasing the number of VGCCs, which have opposing effects on the switching frequency, this non-monotonic trend is observed in the switching frequency.

Effect of calcium pulse failures on switching dynamics

To study the rate-coding properties of the AHP current, we induce calcium pulse failure with a given probability of failure. Higher the failure rate causes fewer calcium pulses, and less regular calcium pulses being integrated by the AHP current. Increasing calcium pulse failure rate decreases the switching frequency as fewer calcium pulses are noted by the AHP open fraction, leading to a slower build-up of AHP current (Fig. 16 (a)) and AHP current has to integrate over more calcium pulses to achieve the threshold current to terminate the burst. Increasing the rate of failures increases the CV of switching increases due to more irregular calcium spikes (Fig. 16 (b)).

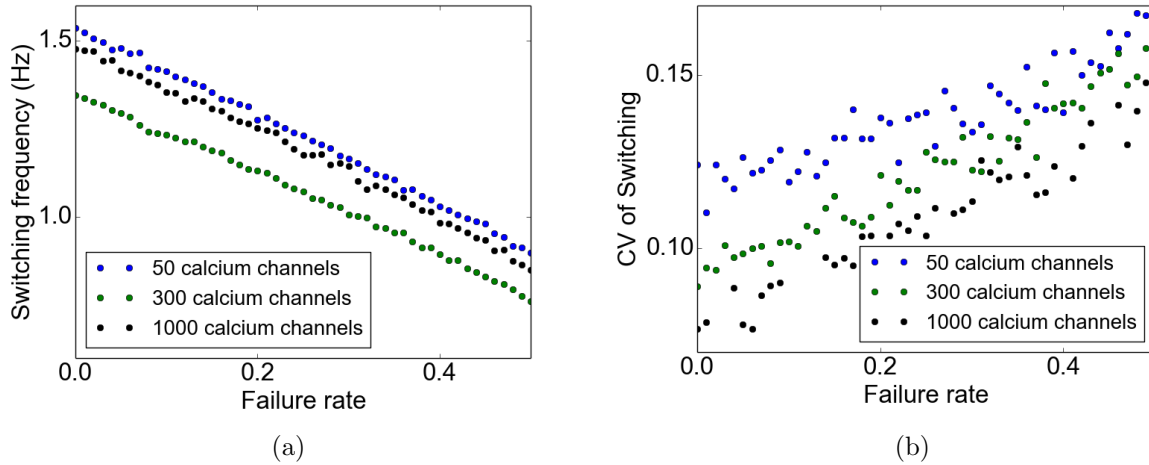
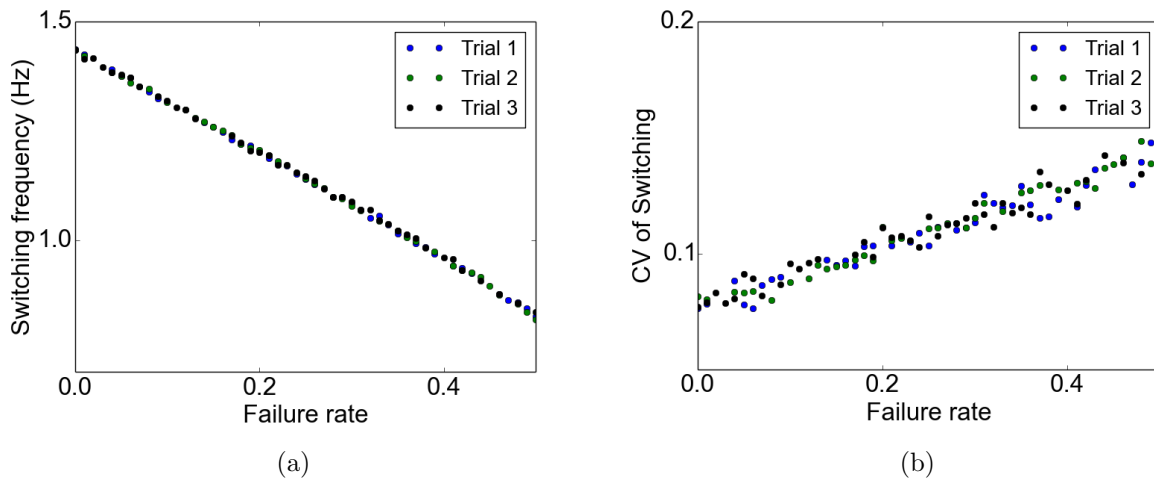


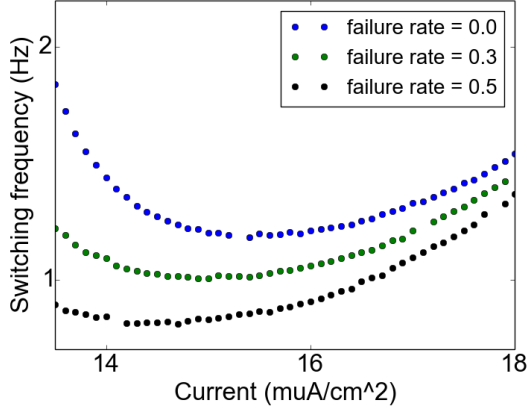
Figure 16: Effect of calcium failures on switching dynamics: (a) The switching frequency decreases on increasing the calcium pulse rates for different channel numbers. (b) The CV of IBI for changing failure rates.

There is a linear decrease in switching frequency with increasing the failure rate, and a similar trend is seen for various random instantiations of the calcium pulse failures occurring anywhere during the epoch of the burst. This indicates that AHP current is counting the number of calcium pulses and can be insensitive to the temporal order of the calcium pulses. This result needs to be further rigorously tested.

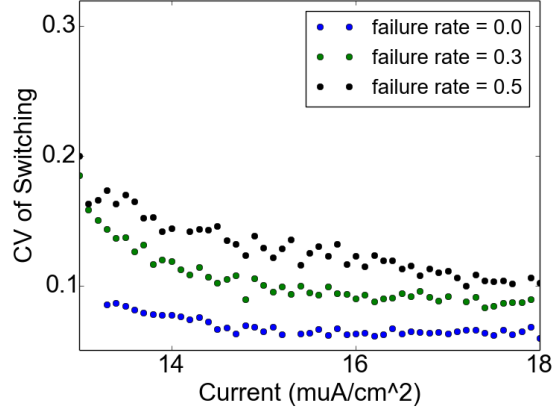


Switching dynamics at three trials of calcium pulse failures. (a) The mean switching frequency for changing three different trials of calcium pulse failures for various failure rate.. (b) The CV of interburst intervals for different failure rates.

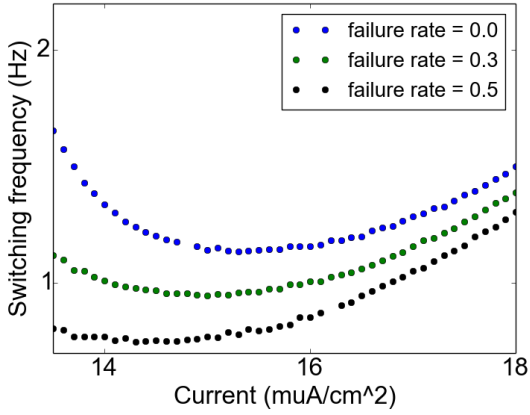
Changing external current with the stochastic calcium has the same effect (Fig. 17) as changing the external current with the deterministic model (Fig 12, 13). The switching frequency is non-monotonically dependent on the external current and higher the failure rate lower the switching frequency. (Fig 17 (a,c,e)). The CVs of switchings show a minimum at intermediate current values for different numbers of ion channels and failure rates.



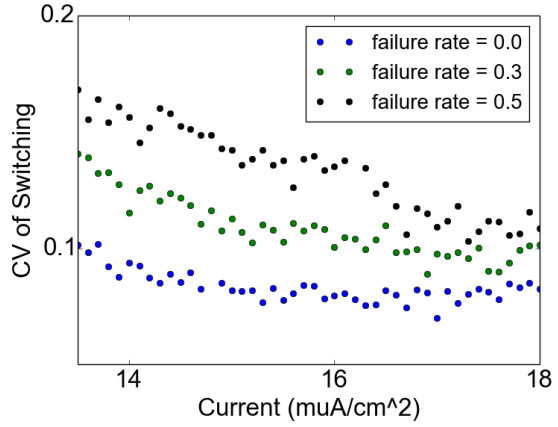
(c) 1000 channels



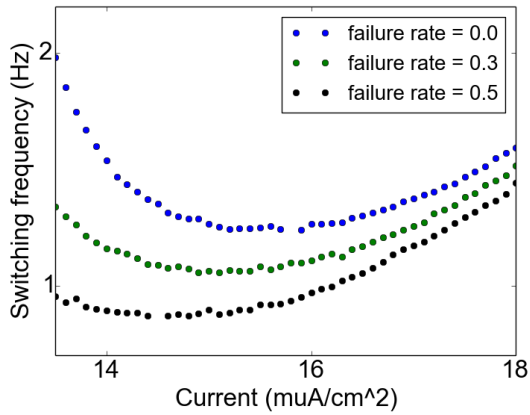
(d) 1000 channels



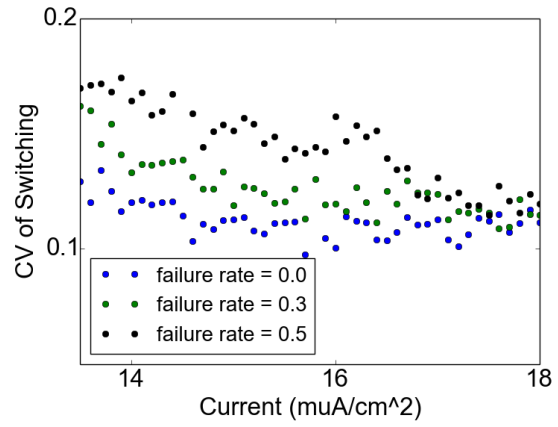
(e) 300 channels



(f) 300 channels



(g) 50 channels



(h) 50 channels

Figure 17: Effect of increasing current on switching dynamics with different failure rates: (a),(c),(d) show the effect of increasing current on the switching frequency for different numbers of calcium channels. (b),(d),(f) show how CV changes with increasing current for different failure rates and numbers of calcium channels.

For a fixed failure rate of 0.3, the CV of switching decreases with increasing channel numbers (Fig. 18 (b)). The switching frequencies change non-monotonically with increasing calcium numbers.(Fig. 18 (a))

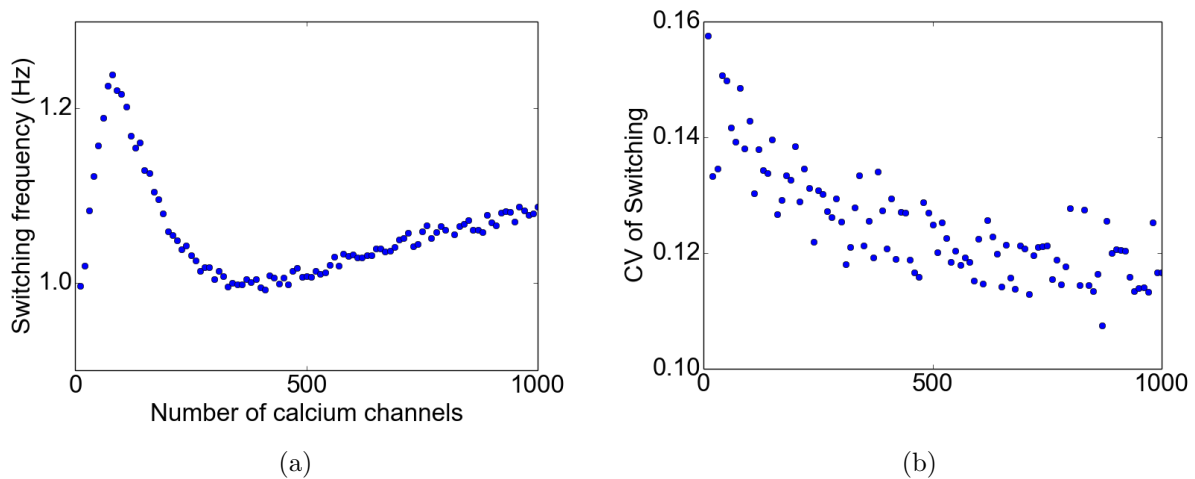


Figure 18: Dynamics at different numbers of calcium channels for a failure rate 0.3 (a) The mean switching frequency for changing the number of calcium channels. (b) The CV of interburst intervals for different numbers of calcium channels.

Effect of calcium channel opening failures on switching dynamics

Inducing individual channel failures decreases the peak calcium coming in through the VGCCs as fewer channels open when an action potential takes place(Fig. 19 (d)). The switching frequency decreases on increasing the per channel failure rate(Fig. 19 (a)). The CV of the inter-burst intervals also decreases with increasing per channel failure rate(Fig. 19 (b)). The peak of the AHP open fraction which terminates the burst reduces on increasing the failure rate (Fig. 19 (c)). The change in open fraction during burst increases as the rate of failure increases. The CV of IBI is proportional to the peak calcium concentration(peak of the open fraction of VGCCs). (Fig. 19 (d)), suggesting and reconfirming that amplitude of pulses and fluctuations is proportional to the CV of IBI. (Fig. 19 (d)) and (Fig. 14 (b)). The decrease in the CV with increasing per channel failure rate remains to be explored, and further study would be done to investigate it.

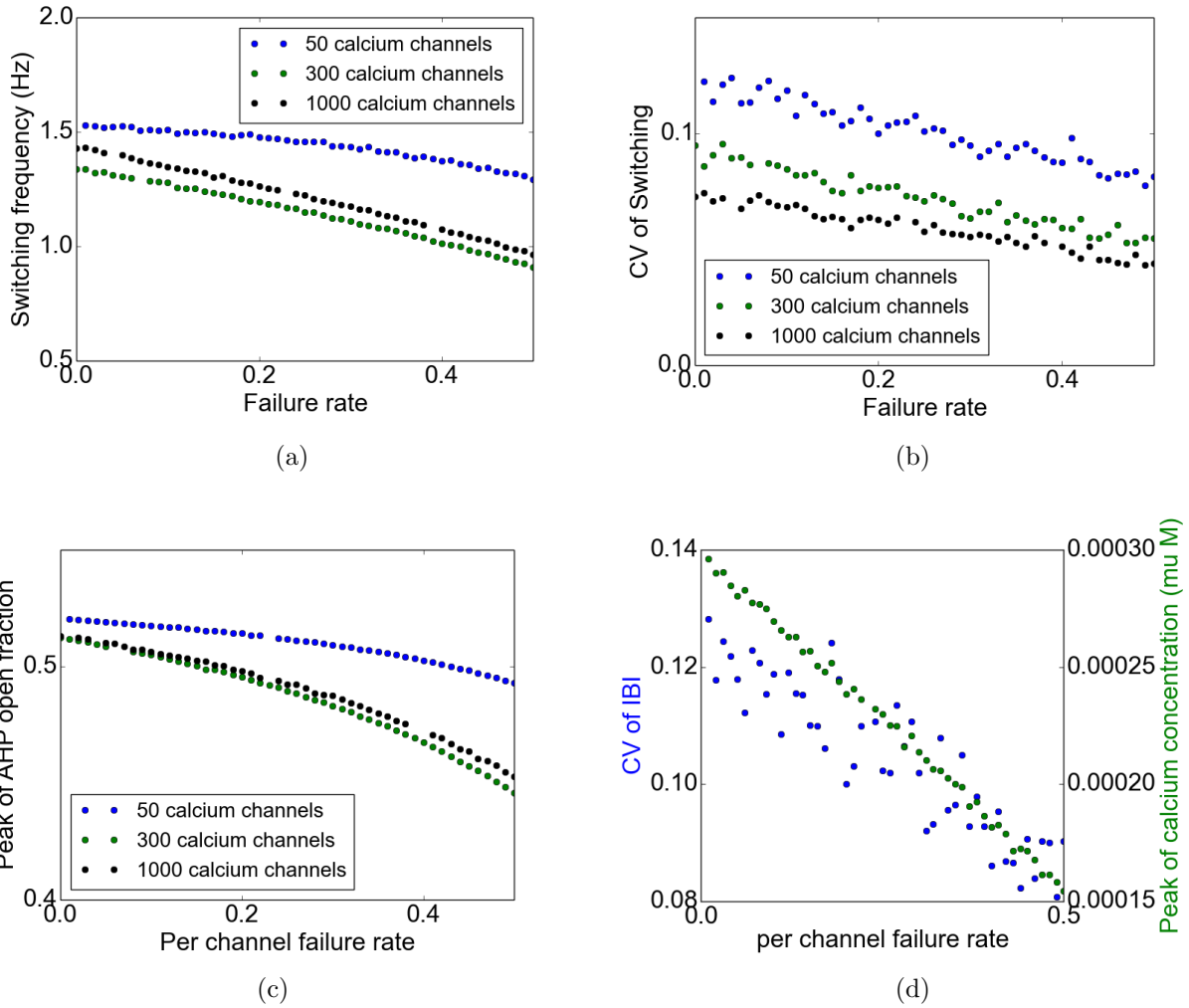


Figure 19: Effect of calcium channel failures on switching dynamics (a) Variation of switching frequency as failure rate is varied. (b) CV of interburst interval for different failure rates. (c) The peak AHP open fraction achieved with changing failure rate. (d) The representative calcium concentration decreases with increasing failure rate.

At a fixed per channel failure rate of 0.3, we see similar switching frequency trend (Fig. 20 (a)) on changing calcium number as seen for no failure (Fig. 15 (a)). The switching frequency is lower because of the lower calcium concentration (Fig. 19 (d)). The CV of switching decreases with increasing channel numbers

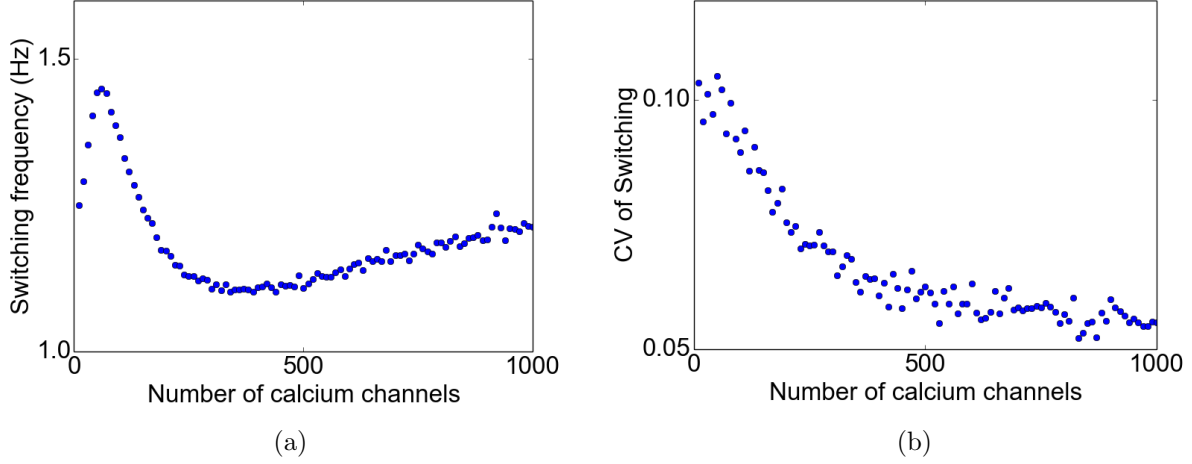


Figure 20: Dynamics at different numbers of calcium channels for a per channel failure rate of 0.3 (a) The mean switching frequency for changing the number of calcium channels. (b) The CV of interburst intervals for different number of calcium channels.

Effect of AHP channel noise on switching dynamics

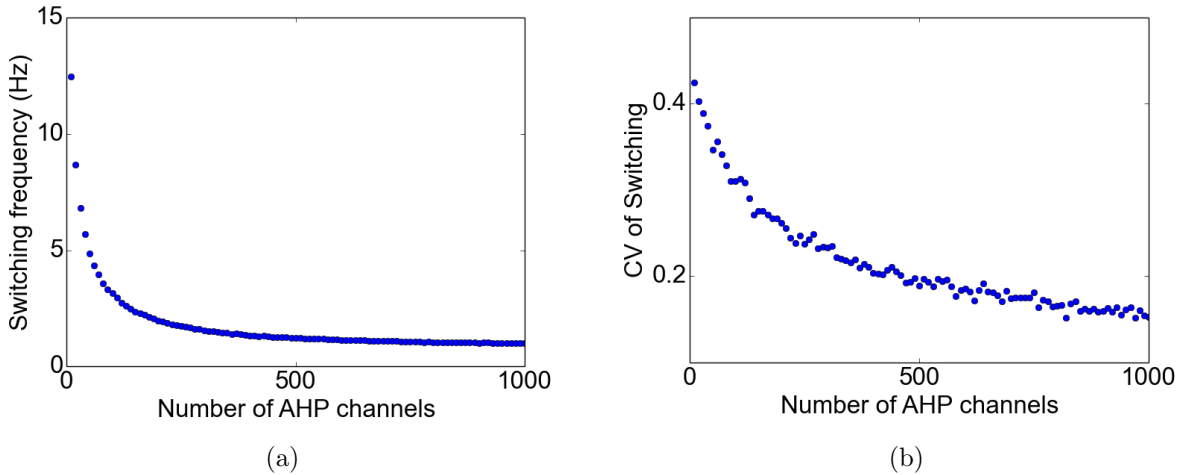


Figure 21: Dynamics at different numbers of AHP channels. (a) The mean switching frequency for changing the number of AHP channels. (b) The CV of interburst intervals for different number of AHP channels.

The switching frequency decreases with increasing the number of AHP channels. There are larger fluctuations which could lead to reaching the threshold current with a small number of random fluctuations when the number of AHP channels are small. As we increase the number of AHP channels the fluctuations in AHP current become smaller and the switching

frequency and the CV decrease on increasing the number of AHP channels.

4 Discussion

In this study, we investigate the effect of different sources of noise on the regularity of the switching of activity in two mutually inhibiting neurons. Previous studies have looked at the regularity of the neuronal firing, oscillations and bursting in the presence of extrinsic noise and in some cases intrinsic noise (McDonnell and Abbott, 2009; Schmid et al., 2001; Wang, 1998; Nesse et al., 2008b,a). We look at both extrinsic and intrinsic noise using a very detailed and accurate implementation of intrinsic channel noise and how it affects the reliable neuronal and network activity. In order to do so, we developed a new algorithm TPG, which we believe accurately captures and simulates the channel fluctuations and different timescales associated with the fluctuations and currents in the neuron.

We show that for the same mean current value, different frequencies and amplitudes of fluctuations affect the mean read-out of the network activity, i.e., switching frequency when slow time-scales are involved. What we hypothesized and now show in this study is that slow decay timescales associated with AHP current integrate over calcium fluctuations to produce regular network activity.

4.1 Extrinsic modulation of switching dynamics

It has been previously shown that various extrinsic factors modulate the switching frequency of two mutually inhibiting neurons (Skinner et al., 1994). Our results show that increasing external current can either increase or decrease the switching frequency (Fig. 12) due to two competing effects of increasing the external current depending on the properties of the AHP current. These biophysical properties such as the channel conductance and calcium binding rates are modulated by neuromodulators (Schwartz et al., 2005). The neurons can achieve different switching dynamics of the network for the same driving current due to the action of neuromodulators. Thus it would be interesting to study the role of 5-HT in maintaining the reliability of the switching (Kozlov et al., 2001).

We see that noise enhances the dynamic range of the network (Fig. 14 (a)) which is in accordance with the previous study (Nesse et al., 2008a) where noise increases the range of switching frequencies by increasing the parameter range which shows switching. In our case widening of the switching frequency happens even without increasing the parameter range over which switching is seen. Thus noise serves as a feature in this system rather than a bug.

We study the effect of changing the driving current, and current noise amplitude on the switching dynamics and find that for certain frequencies of calcium spikes, the network is more robust to current noise, and the switching is more regular (Fig. 13). Robust switchings in the presence of noise over certain frequencies of calcium pulses indicate a match between the calcium spike frequencies, fluctuation time scales, and AHP integration time-scales. These insights suggest that the frequency of calcium spikes and amplitude of calcium fluctuation dictate the reliability of the switching in neurons and AHP current integrates over fluctuations more robustly at certain frequencies to help neurons achieve reliable switching. A similar mechanism via match in timescales of fluctuations and AHP current and slow integrative properties of AHP current could explain the regular switching seen in many systems such as the Lamprey locomotion CPG and pre-Botzinger complex (Nesse et al., 2008b; Cangiano and Grillner, 2004).

4.2 Effect of intrinsic noise

We studied the effect of channel noise from calcium channels and AHP channels on the switching dynamics. With varying calcium channel numbers we saw that the switching frequency is higher (Fig. 15 (a)) for a small number of ion channels due to large channel fluctuations. The higher switching frequency is seen for a range number of calcium channels ($\sim 50 - 300$), which also is a realistic estimate for the number of L-type calcium channels present in the neuron. Such higher switching frequencies could indicate optimal activation the CPGs by noisy calcium currents and could explain why the rat spinal cord locomotor CPG is optimally activated by noisy waveforms (Taccola, 2011). The dependence of the switching frequency on the frequency and amplitude of fluctuations (Fig 15) gives a novel insight that even for a very large number of ion channels when the current fluctuations are smaller, fluctuations cannot be ignored as they change the switching dynamics significantly. Even for very large number of ion channels, the switching frequency is still higher than the deterministic switching frequency due to the highly frequent small fluctuations in the calcium current.

The linear dependence of switching frequency on the failure rate over multiple random instantiations of the pulse failures (Fig. 16), suggests that AHP current can be a pattern insensitive integrator of spike number. It has been shown that slow afterhyperpolarization which arises from Na^{+1}/K^{+1} pump dynamics can act as an integrator of spike number and serve as cellular memory on the time scales of the cycle periods of the locomotion rhythms (Pulver and Griffith, 2010). Also, studies have shown that a short-term memory in the form of changed excitability arises from potassium currents with slow inactivation

(Turrigiano et al., 1996; Marder et al., 1996). It is interesting to investigate if sAHP arising from calcium-mediated potassium channel would give rise to cellular short term memory and pattern insensitive integration of spikes as these channels are implicated in modulating the synaptic plasticity and memory encoding by changing the excitability in hippocampal CA1 Pyramidal cells (Stackman et al., 2002).

We induced single or per calcium channel failures and by varying the per channel failure rate we see that the switching frequency and CV of switchings decreased with increasing failure rate(Fig 19). Increasing the failure rate results in fewer channels being employed and open which results in lower open fraction and lower calcium peak values (Fig 19). Varying the number of channels being employed can change excitability and the spiking threshold of the neuron (White et al., 2000). Thus varying the rate of per channel failure could be changing the excitability of the neuron, and it would be interesting to study it further how changing excitability of neurons could modulate the regularity of the switchings.

It is also interesting to note that the AHP and calcium channel noise affect the switching dynamics differently (Figs. 15, 21). The calcium channel noise does not modulate the switching frequency range as much as the AHP channel noise which suggests that the neurons due to the slow time-scales of AHP current can achieve robustness to the calcium channel noise, which is the biggest source of stochasticity in the neuron to maintain regular switching.

4.3 Tandem Progression Gillespie Algorithm

For stochastic simulations, we used the TPG algorithm to account for all calcium channel fluctuations. Though qualitatively the three algorithms (algorithm no. 1, 2, and 3, as discussed before) show similar switching CV (Fig. 21, 22, 23), in a stochastic-deterministic simulation paradigm it is important to look at the assumptions underlying the accuracy of the method being used. When only one type of channels is modeled using Markovian description, the waiting times given by the Gillespie algorithm will not capture the whole neuronal dynamics, which could lead to missing out on accurately capturing the fluctuations. Previously described methods are valid under the assumption that rates do not change significantly during the waiting time. From unpublished data Mahajan et. al, for a small number of channels, the waiting times are long, and many events take place in the meantime, which would not be taken into account by the channel being modeled using standard Gillespie algorithm. Such a paradigm would not accurately model the effect of stochasticity on the neuronal dynamics. From the external noise simulations, we know that when slow temporal dynamics of ion channels are involved, the fluctuations cannot be ignored as they change the dynamics significantly. Thus to take into account every fluctuation and to evolve the system

at reasonable time intervals so as to not miss the fast neuronal dynamics we use the TPG algorithm.

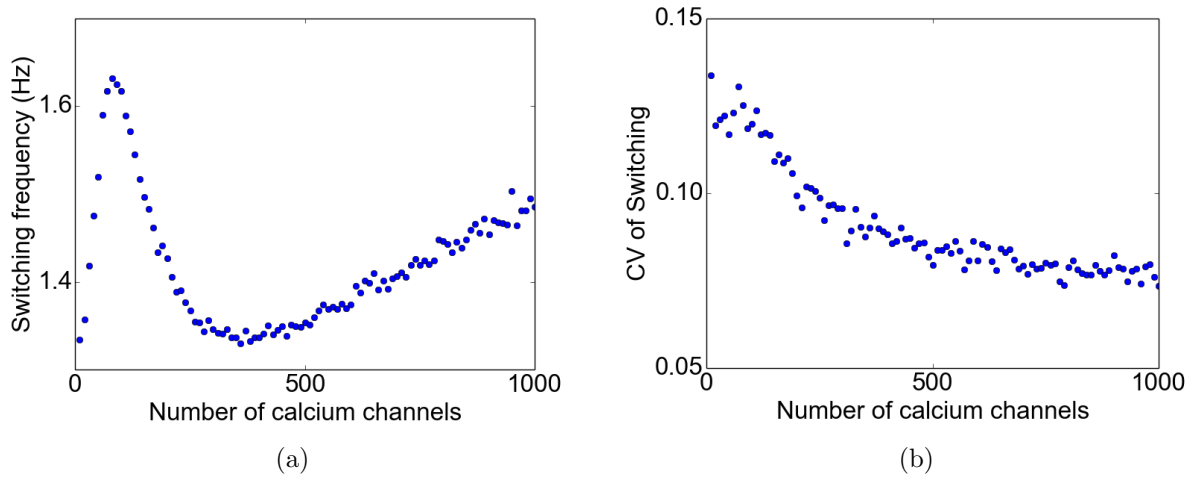


Figure 22: Tandem Progression Gillespie Algorithm: (a) Variation in switching frequency due to changing number of calcium channels (b) CV of inter-burst intervals for different number of calcium channels.

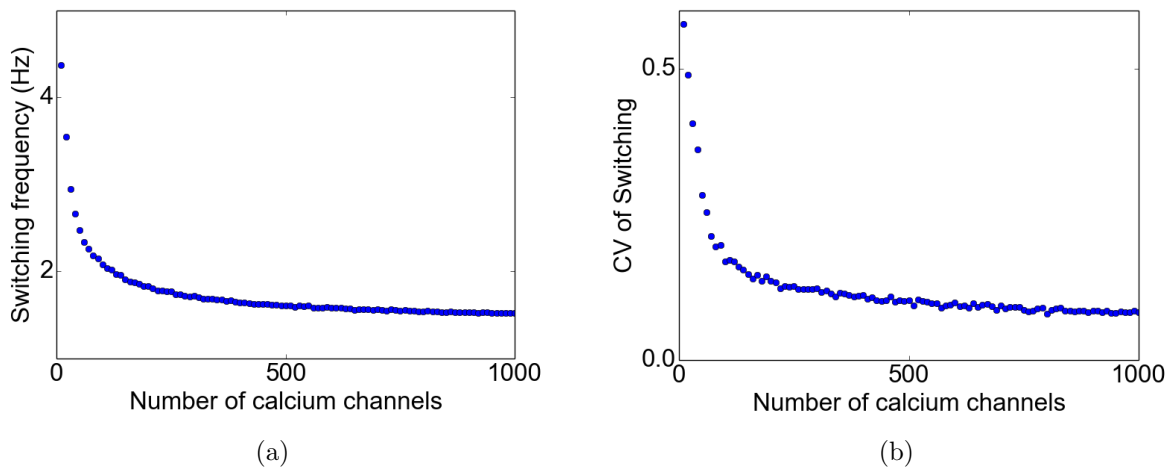


Figure 23: White and Chow Gillespie Algorithm: (a) Variation in switching frequency due to changing number of calcium channels (b) CV of inter-burst intervals for different number of calcium channels.

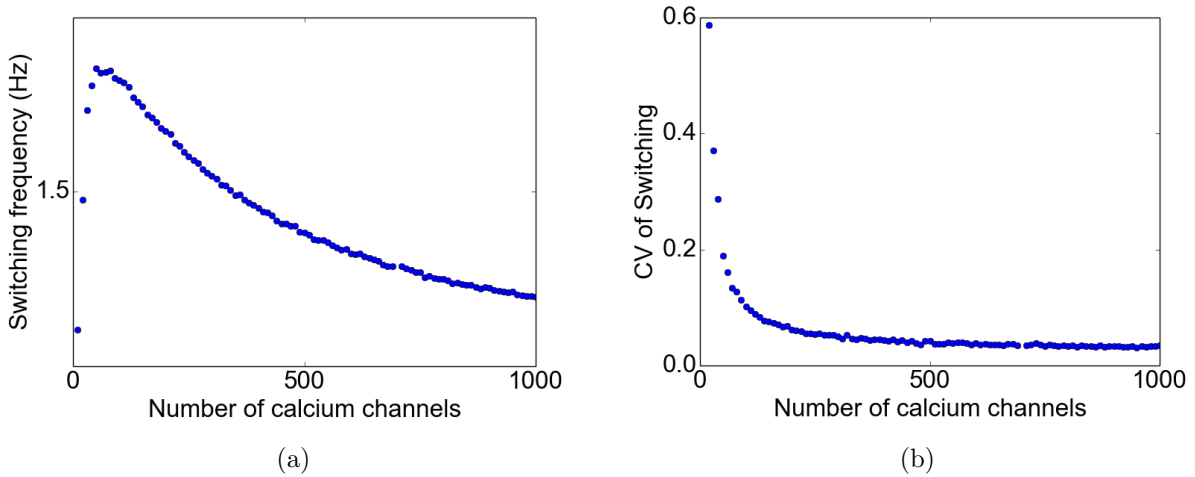


Figure 24: Goldwyn and Shea-Brown Gillespie Algorithm: (a) Variation in switching frequency due to changing the number of calcium channels (b) CV of inter-burst intervals for varying the number of calcium channels.

It is interesting to note though multiple algorithms show lower CV with increasing number of calcium channels, the switching frequency dynamics are different for TPG (when all fluctuations are taken into account) compared to the other algorithms(Fig 22,23,24 (a)). The CVs of switching are lower for small channel numbers for simulations using TPG compared to other methods (Fig 22,23,24 (b)). We believe that TPG algorithm simulates the stochastic dynamics accurately and we are testing the accuracy of the algorithm rigorously. The lower CV for a small number of ion channels (Fig 22,23,24 (b)) seen in the case of TPG compared to other algorithms, i.e. when fluctuations are taken into accurately, further strengthens our result that indeed the slow timescales of AHP are able to integrate over stochastic current signals coming in from small number of ion channels in order to achieve reliable switching.

In conclusion, we see that for optimal frequencies of calcium current and fluctuations, the slow decay time scales of AHP current enable the neurons to produce regular switching behavior. The new insights that we gained from this study would help in understanding how neuronal networks achieve robustness to noise and help in understanding effects of noise and accurately modeling noise in a wide variety of systems.

4.4 Future directions

We want to expand our model into the Lamprey locomotion CPG to study the effect of intrinsic and extrinsic noise on the locomotion dynamics using insights from the present study (Kozlov et al., 2001).

Our preliminary simulations suggest cumulative recruitment of open sAHP channels for a range of intrinsic noise amplitudes driven by stochastic fast timescales of opening relative to a slower closing rate. We want to explore if this could be a competitive mechanism that could lead to eventual faster motion instead of recruiting more neurons.

We want to investigate if sAHP arising from calcium-mediated potassium channel would give rise to cellular short term memory by changing the excitability for the neuron. We want to study how noise modulates the information content in the burst (Izhikevich et al., 2003). As our results suggest that AHP can act as a pattern insensitive integrator of spikes, we want to explore the rate coding properties of this AHP current.

5 References

References

- Cangiano, L. and Grillner, S. (2004). Mechanisms of Rhythm Generation in the Lamprey Locomotor Network. Number 1680.
- Chow, C. C. and White, J. a. (1996). Spontaneous action potentials due to channel fluctuations. *Biophysical journal* *71*, 3013–3021.
- Daun, S., Rubin, J. E. and Rybak, I. A. (2009). Control of oscillation periods and phase durations in half-center central pattern generators: A comparative mechanistic analysis. *Journal of Computational Neuroscience* *27*, 3–36.
- Fox, R. F. and Lu, Y. N. (1994). Emergent collective behavior in large numbers of globally coupled independently stochastic ion channels. *Physical Review E* *49*, 3421–3431.
- Gillespie, D. T. (1976). A general method for numerically simulating the stochastic time evolution of coupled chemical reactions. *Journal of Computational Physics* *22*, 403–434.
- Goldwyn, J. H. and Shea-Brown, E. (2011). The what and where of adding channel noise to the Hodgkin-Huxley equations. *PLoS Computational Biology* *7*.
- Hodgkin, A. L. and Huxley, A. F. (1990). A quantitative description of membrane current and its application to conduction and excitation in nerve. *Bulletin of Mathematical Biology* *52*, 25–71.

- Izhikevich, E. M., Desai, N. S., Walcott, E. C. and Hoppensteadt, F. C. (2003). Bursts as a unit of neural information: Selective communication via resonance. *Trends in Neurosciences* *26*, 161–167.
- Kozlov, A., Kotaleski, J. H., Aurell, E., Grillner, S. and Lansner, A. (2001). Modeling of substance P and 5-HT induced synaptic plasticity in the lamprey spinal CPG: Consequences for network pattern generation. *Journal of Computational Neuroscience* *11*, 183–200.
- Lu, J., Sherman, D., Devor, M. and Saper, C. B. (2006). A putative flip-flop switch for control of REM sleep. *Nature* *441*, 589–94.
- Manira, A., Tegner, J., Grillner, S. and Manira, A. E. L. (2013). Calcium-dependent potassium channels play a critical role for burst termination in the locomotor network in lamprey. *Calcium-Dependent Potassium Channels Play a Critical Role for Burst Termination in the Locomotor Network in Lamprey.* *72*, 1852–1861.
- Marder, E., Abbott, L. F., Turrigiano, G. G., Liu, Z. and Golowasch, J. (1996). Memory from the dynamics of intrinsic membrane currents. *Proceedings of the National Academy of Sciences of the United States of America* *93*, 13481–13486.
- McDonnell, M. D. and Abbott, D. (2009). What is stochastic resonance? Definitions, misconceptions, debates, and its relevance to biology. *PLoS Computational Biology* *5*.
- Modchang, C., Nadkarni, S., Bartol, T. M., Triampo, W., Sejnowski, T. J., Levine, H. and Rappel, W.-J. (2010). A comparison of deterministic and stochastic simulations of neuronal vesicle release models. *Physical biology* *7*, 026008.
- Myre, C. D. and Woodward, D. J. (1993). Bistability, switches and working memory in a two-neuron inhibitory-feedback model. *Biological Cybernetics* *68*, 441–449.
- Nesse, W. H., Borisyuk, A. and Bressloff, P. C. (2008a). Fluctuation-driven rhythmogenesis in an excitatory neuronal network with slow adaptation. *Journal of Computational Neuroscience* *25*, 317–333.
- Nesse, W. H., Del Negro, C. A. and Bressloff, P. C. (2008b). Oscillation regularity in noise-driven excitable systems with multi-time-scale adaptation. *Physical Review Letters* *101*, 3–6.
- Otto Friesen, W. (1994). Reciprocal inhibition: A mechanism underlying oscillatory animal movements. *Neuroscience and Biobehavioral Reviews* *18*, 547–553.

- Pulver, S. R. and Griffith, L. C. (2010). Spike integration and cellular memory in a rhythmic network from Na^+/K^+ pump current dynamics. *Nature neuroscience* 13, 53–9.
- Sah, P. and Clements, J. D. (1999). Photolytic manipulation of $[\text{Ca}^{2+}]_i$ reveals slow kinetics of potassium channels underlying the afterhyperpolarization in hippocampal pyramidal neurons. *The Journal of neuroscience : the official journal of the Society for Neuroscience* 19, 3657–3664.
- Schmid, G., Goychuk, I. and Hänggi, P. (2001). Stochastic resonance as a collective property of ion channel assemblies. *Europhysics Letters (EPL)* 56, 22–28.
- Schwartz, E. J., Gerachshenko, T. and Alford, S. (2005). 5-HT prolongs ventral root bursting via presynaptic inhibition of synaptic activity during fictive locomotion in lamprey. *Journal of neurophysiology* 93, 980–8.
- Skinner, F. K., Kopell, N. and Marder, E. (1994). Mechanisms for oscillation and frequency control in reciprocally inhibitory model neural networks. *Journal of Computational Neuroscience* 1, 69–87.
- Stackman, R. W., Hammond, R. S., Linardatos, E., Gerlach, A., Maylie, J., Adelman, J. P. and Tzounopoulos, T. (2002). Small conductance Ca^{2+} -activated K^+ channels modulate synaptic plasticity and memory encoding. *Journal of neuroscience* 22, 10163–10171.
- Stanley, D. A., Bardakjian, B. L., Spano, M. L. and Ditto, W. L. (2011). Stochastic amplification of calcium-activated potassium currents in Ca^{2+} microdomains. *Journal of Computational Neuroscience* 31, 647–666.
- Taccola, G. (2011). The locomotor central pattern generator of the rat spinal cord in vitro is optimally activated by noisy dorsal root waveforms. *Journal of neurophysiology* 106, 872–84.
- Tegnér, J., Hellgren-Kotaleski, J., Lansner, A. and Grillner, S. (1997). Low-voltage-activated calcium channels in the lamprey locomotor network: simulation and experiment. *Journal of neurophysiology* 77, 1795–1812.
- Turrigiano, G. G., Marder, E. and Abbott, L. F. (1996). Cellular short-term memory from a slow potassium conductance. *Journal of neurophysiology* 75, 963–6.
- Wang, X.-J. (1998). Calcium coding and adaptive temporal computation in cortical pyramidal neurons. *J Neurophysiol* 79, 1549–1566.

White, J. A., Rubinstein, J. T. and Kay, A. R. (2000). Channel noise in neurons. *Trends in Neurosciences* 23, 131–137.

6 Appendix

Effect of varying r_b at different noise amplitudes.

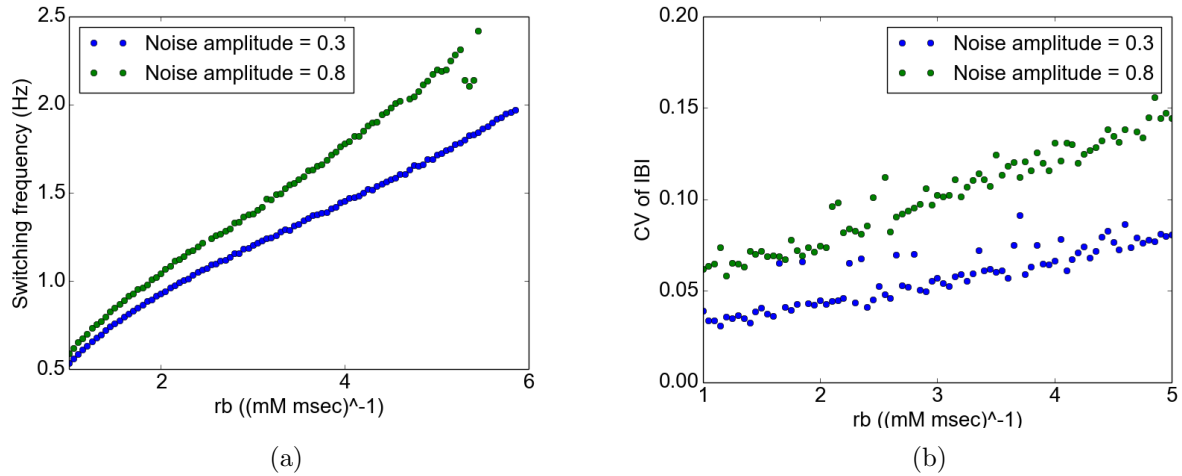


Figure 25: r_b and noise: (a) Switching frequency as a function of r_b for different noise levels. (b) CV of IBI for different r_b values.

At resting membrane potential the fluctuations in the open fractions die down as number of calcium channels are increased.

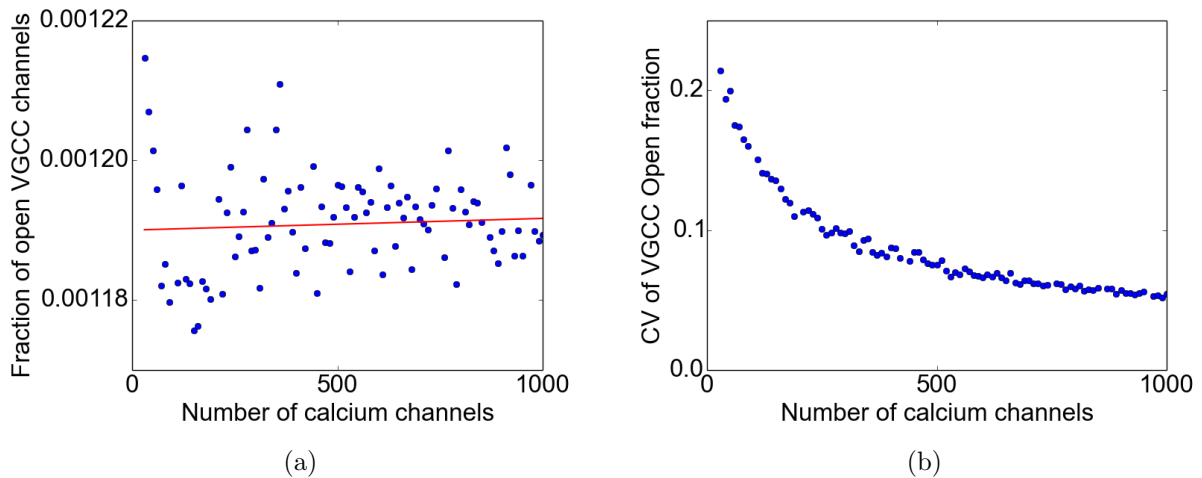
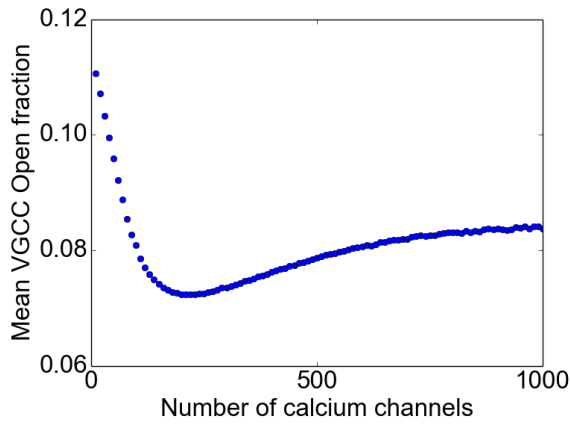
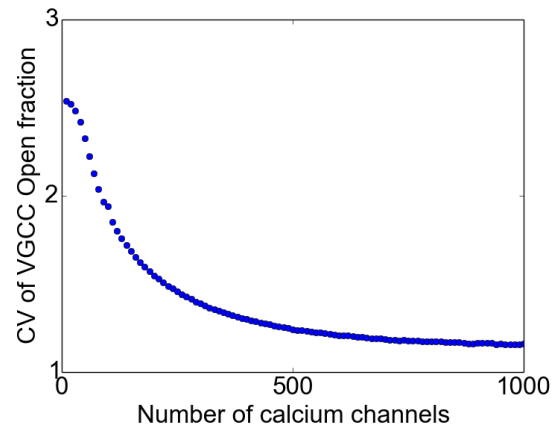


Figure 26: Resting voltage dynamics: (a) The open fraction of VGCCs at $V = -65$ mV for different numbers of calcium channels (b) CV of open fraction decreases as number of calcium channels increase.

VGCC dynamics of unconnected neuron at different channel numbers.



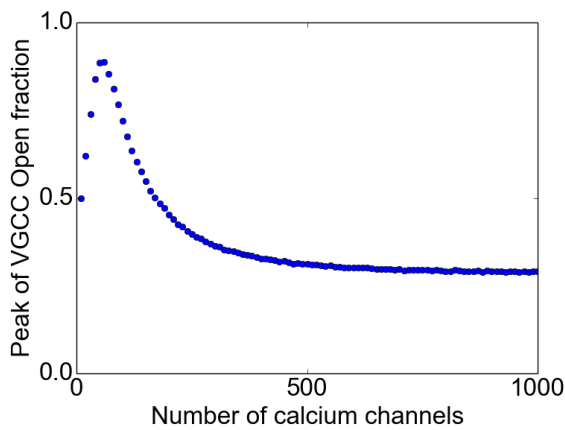
(a)



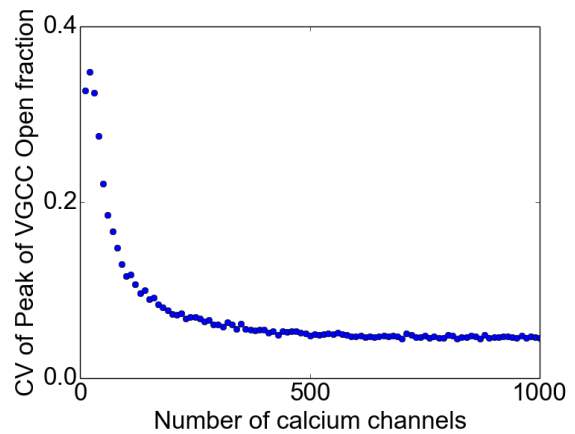
(b)

Figure 27: Unconnected neuron stochastic dynamics: (a) The mean open fraction of VGCCs for different numbers of calcium channels (b) CV of open fraction decreases as number of calcium channels increase.

VGCC dynamics of connected neuron at different channel numbers.



(a)



(b)

Figure 28: Connected neuron stochastic VGCC dynamics: (a) The peak of open fraction of VGCCs for different numbers of calcium channels (b) CV of open fraction peak decreases as number of calcium channels increase.